eLife

Reviewed Preprint
v2 • January 21, 2025
Revised by authors

Reviewed Preprint
v1 • January 11, 2024

Neuroscience

Genetic and pharmacologic alterations of claudin9 levels suffice to induce functional and mature inner hair cells

Yingying Chen, Jeong Han Lee, Jin Li, Seojin Park, Maria C Perez Flores, Braulio Peguero, Jennifer Kersigo, Mincheol Kang, Jinsil Choi, Lauren Levine, Michael Anne Gratton, Bernd Fritzsch, Ebenezer N Yamoah

University of Nevada, Reno, School of Medicine, Department of Physiology and Cell Biology, Reno, United States • Indiana University School of Medicine, Department of Pharmacology and Toxicology, Indianapolis, United States • Department of Otolaryngology, University of Washington, Seattle, United States • Prestige Biopharma, Busan, Republic of Korea • University of Iowa, Department of Biology, Iowa City, United States • Boys town National Research Hospital, Omaha, United States • Washington University, Program in Audiology and Communication Sciences, Seattle, United States

eLife Assessment

This **valuable** study reports the induction of supernumerary inner hair cells in the mouse cochlea upon reducing the expression level of a tight-junction protein (claudin-9) at developmental stages. Although these ectopic hair cells are functional and persists through adulthood, the evidence supporting some of the claims is **incomplete**, particularly regarding the underlying mechanisms of cell differentiation and the potential of the approach for hair-cell regeneration. The work will be of interest to scientists working in the development and regeneration of hair cells in the inner ear.

https://doi.org/10.7554/eLife.92877.2.sa4

Abstract

Hearing loss is the most common form of sensory deficit. It occurs predominantly due to hair cell (HC) loss. Mammalian HCs are terminally differentiated by birth, making HC loss challenging to replace. Here, we show the pharmacogenetic downregulation of *Cldn9*, a tight junction protein, generates robust supernumerary inner HCs (IHCs) in mice. The ectopic IHC shared functional and synaptic features akin to typical IHCs and were surprisingly and remarkably preserved for at least fifteen months >50% of the mouse's life cycle. *In vivo*, *Cldn9* knockdown using shRNA on postnatal days (P) P2-7 yielded analogous functional ectopic IHCs that were equally durably conserved. The findings suggest that Cldn9 levels coordinate embryonic and postnatal HC differentiation, making it a viable target for altering IHC development pre- and post-terminal differentiation.

Introduction

Mammalian cochlear hair cells (HCs) comprise a single row of inner hair cells (IHCs) and three rows of outer hair cells (OHCs). HCs transduce sound-mediated mechanical force into neural electrical codes for ear-brain intercommunication. The IHCs are the predominant afferent transducers, while the OHCs amplify low-level sound. Mammalian HCs are terminally differentiated by birth, and they are susceptible to damage by ototoxic drugs, noise-overexposure, aging, and environmental insults, resulting in hearing loss, the most common sensory deficit (Neitzel and Fligor, 2019; Rybak and Ramkumar, 2007; Wilson and Tucci, 2021; Wu et al., 2020). Emerging understanding of the mechanisms of transcription factors that induce HC differentiation (Atkinson et al., 2014; Bermingham et al., 1999; Garcia-Anoveros et al., 2022; Zheng and Gao, 2000), and potential induction for regeneration are promising, but none have produced new HCs with sustained functions (Iyer et al., 2022b; Zine et al., 2021). Thus, the current treatment for hearing loss ensuing from HC loss is cochlear implants, despite the potential advantages of HC-replacement therapy (Hinton et al., 2021; Sullivan et al., 2020).

In the mammalian cochlea, each HC is separated from the next by intervening supporting cells (SCs), forming an invariant and alternating mosaic along the cochlea's length. Cochlear SCs can divide and trans-differentiate into HCs in the neonatal stage, serving as a potential resource for HC differentiation using transcription and developmental signaling factors (White et al., 2006). At the neonatal stage, *Atoh1*, a basic helix-loop-helix factor, induces SCs trans-differentiation into HCs. Upregulation of *Atoh1*, *GFI1*, and *POU4F3* triggers HC differentiation, but the fledgling HCs invariably degenerate, suggesting pre-maturity (Iyer et al., 2022a; Liu et al., 2012). Additionally, inhibition of the Notch signaling or upregulation of the wnt1 pathway suffices to drive HC formation from SCs (Tang et al., 2023), but the functional features of the newly developed HCs are circumspect (Mizutari et al., 2013; Waqas et al., 2016). While transcription factors are potent targets for developmental regulation, a cadre of these essential DNA-binding proteins and the precise timing of expression are required to complete the developmental cascade (Jahan et al., 2015). Thus, the key is identifying HC-developing bands of transcription and signaling factors to treat hearing loss. Recent studies identified the transcription factors INSM1 and IKZF2 as the regulators of OHC fate, while the transcription factor TBX2 specifies and maintains HC and SC fate (Kaiser et al., 2022; Li et al., 2023), advancing understanding of HC-subtype developmental specification mechanisms.

Contact-mediated lateral inhibition is among the final developmental events, where once a cell fate is determined, it inhibits neighboring cells from becoming that cell type. The HC-SC interphase is laced with tight junction proteins (TJPs), which may mediate lateral inhibition mechanisms in nonmammalian vertebrates, though their additional function is unclear in mammals (Chrysostomou et al., 2012; Goodyear and Richardson, 1997; Petrovic et al., 2014). In addition, TJPs were also found to regulate cell proliferation (Bhat et al., 2020; Díaz-Coránguez et al., 2019). The TJP scaffold cingulin regulates lateral inhibition in HC-SC rearrangements in the avian basilar papilla (Goodyear and Richardson, 1997), and claudin b (*cldnb*), an ortholog of the *cldn4* in humans, upregulation controls cellular patterning during HC regeneration in zebrafish (Montalbano et al., 2021). Moreover, damaged HC extrusion and the breaking of intercellular junctional adhesions may trigger differentiation and regenerative proliferation (Corwin et al., 2007). In mammals, E-cadherin's junctional expression negatively alters HC regenerative capacity (Burns et al., 2008; Burns et al., 2013), while *Cldn9* is a positive regulator of cell proliferation (Hong et al., 2014; Zavala-Zendejas et al., 2011). Although the high expression of *Cldn9* in the organ of Corti (OC) is well-established (Kudo et al., 2018; Nakano et al., 2009) (**Fig. 1A-C**), it is unknown whether regulation of the TJP contributes to sensory cell differentiation.

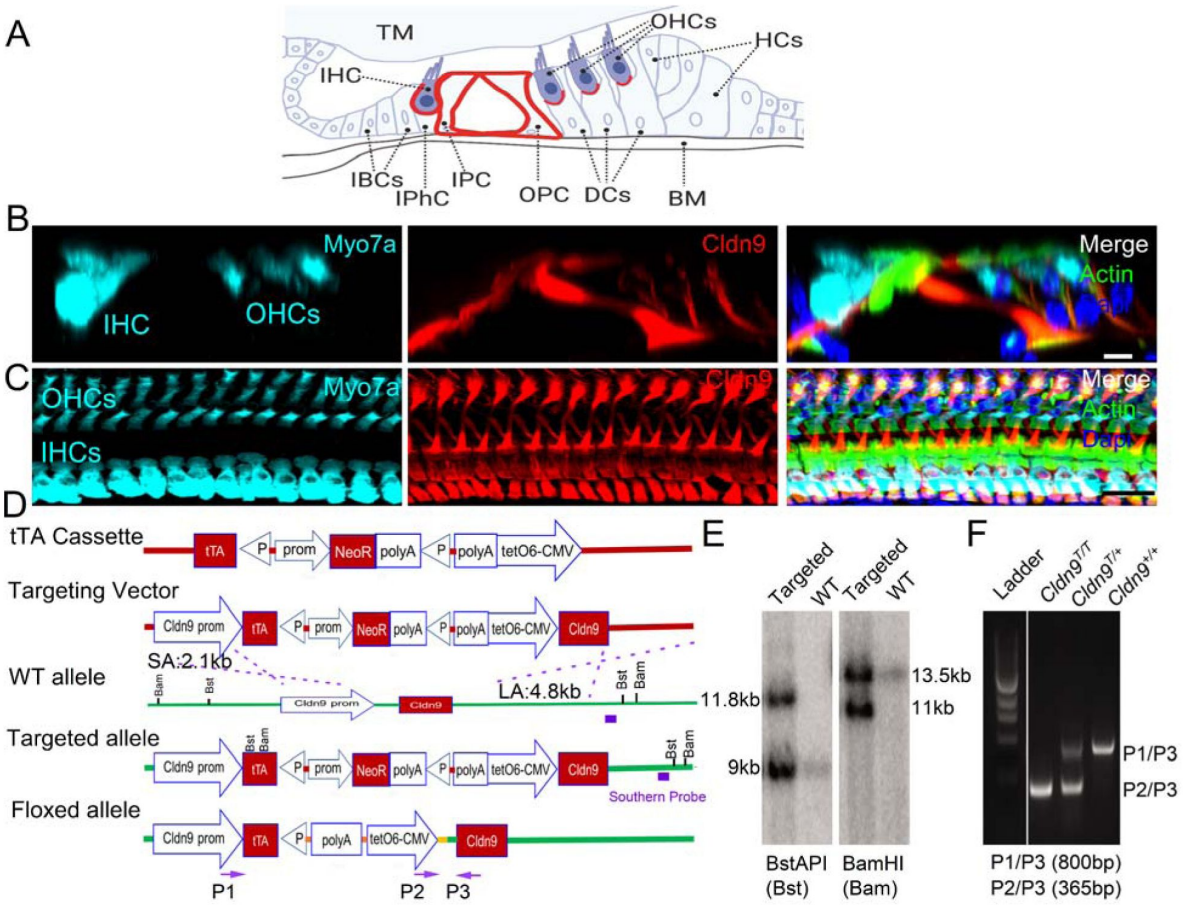

Figure 1.

The cochlear partition and construct of doxycycline-tet-OFF-*Cldn9* mouse line.

A. Schematic diagram of the radial section of the cochlear partition. The organ of Corti (OC) is seated on the basilar membrane (BM). The inner and outer pillar cells (IPC and OPC) are separated from the inner and outer hair cells (IHC, OHCs) by tight junction proteins (TJPs). The red lines indicate the expression outline of Cldn9. TM: tectorial membrane; IHC: inner hair cell; OHCs: outer hair cells; IBC: inner border cell; IPhC: inner phalangeal cell; IPC: inner pillar cell; DCs: Deiters cells; HCs: Hensen's cells. **B.** The immunostaining of *Cldn9* in the 8-wk old WT (*Cldn9*$^{+/+}$) mouse cochlea showing IHC stained with myosin7a (cyan) and claudin9 (red)antibodies, phalloidin, actin (green) for stereocilia bundles and Dapi (blue) for nuclear stain. **C**. Surface view of the cochlea **B**. Scale = 10 μm. **D.** The construct of Doxycycline-tet-OFF- *Cldn9* in the ES cells. Generation of a genetically modified mouse line in which the level of *Cldn9* gene expression can be regulated by doxycycline: A tetracycline-based genetic switch (tTA cassette) consists of three main modules, the tetracycline-controlled transcriptional activator (tTA), the neomycin resistance gene flanked by LoxP sites, and the final module that contains six copies of the tet operator (tetO) fused to the minimal CMV promoter. The tTA cassette was inserted at the −110-nucleotide position upstream of the translational start of *Cldn9* to generate the targeting vector. The targeting vector was electroporated into B6 mouse embryonic stem cells. Following the selection in G418, DNA samples from the neomycin-resistant ES cell clones were prepared for short-arm PCR/sequencing analysis and Southern blot analysis to confirm the insertion of the tTA cassette in the ES cells. The genetically modified ES cells containing one copy of the tTA cassette were injected into the healthy albino B6 blastocysts, and the injected blastocysts were transplanted into the uterus of an albino B6 mouse to generate the chimeric mouse. The chimeric mouse was then bred with albino B6 mice to produce the F1 heterozygous mouse, and the germline transmission was confirmed by tail DNA genotyping. The deletion of the selection marker in the tTA cassette by crossing the F1 mouse with the embryonic Cre line (B6.129S4-Meox2 tm1(cre)Sor /J). **E**. Genomic DNA samples were prepared from neomycin-resistant ES cell clones and digested with BstAPI or BamHI. The tTA cassette insertion was confirmed by the Southern blot analysis. **F**. Mouse tail DNA genotyping was carried out using primers P1/P3 for WT and P2/P3 for targeted alleles showing *Cldn9*$^{T/T}$, *Cldn9*$^{T/+}$ and *Cldn9*$^{+/+}$samples.

To determine the roles in vivo of Cldn9, we generated doxycycline (dox)-tet-OFF-Cldn9 transgenic mice to regulate expression levels of Cldn9. The downregulation of Cldn9 resulted in functional supernumerary (ectopic) putative IHCs along the cochlear contour. Auditory neurons innervated ectopic mechanically transducing IHCs with synaptic features resembling normal IHCs. Analogous additional putative IHCs differentiation was observed when Cldn9-shRNA was injected through the round window to postnatal (P) days (P2, P4, and P7) mice, suggesting that regulation of Cldn9 levels coordinates embryonic and postnatal development differentiation of SC into IHCs. Notably, the ectopic IHCs at the apical and middle-frequency contour of the cochlea were preserved for over half the mouse's life cycle (15 months), making Cldn9 a viable target for generating supernumerary IHCs.

Results

To control *Cldn9* levels *in vivo*, we generated a mouse model with a site-specific genetic switch regulated by dietary doxycycline (dox) and dox-containing drinking water without interfering with the typical profile of *Cldn9* expression ((Supplement figure 1 (**S1**)). **Figures 1D-F** show the design constructs and Southern blot analysis to confirm the insertion cassette in the ES cells. The genotyping was performed using PCR with the tail tissue. Transgene was generated on mixed C57/B6 and backcrossed into a CBA-CaJ (CBA) background after 12 generations to reduce accelerated progressive hearing loss (Peguero and Tempel, 2015; Sergeyenko et al., 2013; Willott and Erway, 1998). Results of quantitative RT-PCR from the three groups of animals, including wild-type littermates ($Cldn9^{+/+}$), heterozygote ($Cldn9^{+/T}$), and homozygous ($Cldn9^{T/T}$) with (1 mg/ml) and without dox treatment. Without dox treatment, $Cldn9^{T/T}$ and $Cldn9^{+/T}$mice demonstrate ~55 and a 40-fold increase in *Cldn9* mRNA expression in cochlear tissue compared with $Cldn9^{+/+}$ cochleae (**S2**). Treatment of $Cldn9^{+/T}$ mice with dox (1 mg/ml) resulted in an ~0.4-0.6-fold decline in mRNA levels compared to $Cldn9^{+/+}$ cochleae (**S2**), translating to a marked difference in Cldn9 protein expression (**S2**). Immunoelectron microscopic analysis showed that Cldn9 levels reduced by ~8-fold in the $Cldn9^{+/T}$ cochlea (**S3**). The $Cldn9^{T/T}$ mice had a reduced survival rate (1.5±0.3 months) relative to the $Cldn9^{+/T}$ littermates (23±2 months). Thus, all experiments were restricted to $Cldn9^{+/T}$ *and* $Cldn9^{+/+}$ littermates fed on dox-water (1 mg/ml). There were no recognizable differences in body weight between $Cldn9^{+/T}$ and $Cldn9^{+/+}$ mice for both females and males (**S2**). All animals were in the CBA background. *Cldn9* downregulation in the $Cldn9^{+/T}$ cochlea showed a qualitative decrease in the Cldn6 and an increase in ILDR1 TJP levels but no comparative differences in others (Kitajiri et al., 2004; Kitajiri and Katsuno, 2016) (**S4**).

Downregulation of *Cldn9* induces the production of ectopic cochlear HCs

5-week-old mice $Cldn9^{+/T}$ cochleae displayed a notable row of ectopic HCs (**Fig. 2A-E**). The ectopic HCs were observed along the cochlear contour, ranged in abundance from base to apex (**S5**), and had contact with innervating neurons, shown in cochlear sections (**Fig. 2A**). The ectopic HCs were positively labeled with anti-myosin VIIa antibody and phalloidin-labeled stereocilia bundles, which are features of typical HCs. Moreover, the ectopic HCs were not labeled with antibodies to prestin (**S6**), a marker for OHCs, suggesting the new HCs were likely derived from the IHC lineage. A distinctive "U"-shaped IHC bundle was apparent (**Fig. 2D**). Scanning electron microscopic (SEM) was used for high-resolution analyses to evaluate IHC and their bundle morphology. The original and ectopic IHCs in $Cldn9^{+/T}$mice had normal morphology, including intact hair bundles (**Fig. 2E**). However, the stereocilia bundle orientation was less orderly when compared to those in $Cldn9^{+/+}$ cochlea (**Fig. 2D-E**). In addition to their shape, the ectopic HCs expressed multiple CtBP2 labeled synaptic structures in contrast to typical OHCs (**Figs. 3B**, **5B**), and reacted positively to otoferlin antibodies (Pangrsic et al., 2010; Roux et al., 2006; Strenzke et al., 2016) (data not shown). We denote the new HCs as "ectopic" IHCs. IHC counts at

different ages (P2-P21) and the cochlear frequency segments (8 kHz and 32 kHz) demonstrate that the *Cldn9*-induced ectopic IHCs were most prominent at the cochlear apex but remained statistically significant at the base (**Figs 2E-F**). Viable ectopic IHCs were identified in 15-month $Cldn9^{+/T}$ mice in the apical cochlea (**Fig. 3**). For OHCs, the numbers along the cochlear contour, apex, middle, and base were not significantly different among the two genotypes at P14 (**S7A**) and at the apical turn of organ of Corti in 15-month-old $Cldn9^{+/T}$ mice (**S7B**).

Functional features of *Cldn9*-induced ectopic IHCs resemble normal IHCs

Motor responses of both mouse genotypes' ($Cldn9^{+/+}$ and $Cldn9^{+/T}$) to auditory stimuli (Preyer's test) were normal. To evaluate the status of IHC function, we analyzed auditory brainstem responses (ABR) to various sound-pressure levels. $Cldn9^{+/T}$mice responses exhibited similar characteristic responses to broadband clicks and pure tones at 8, 16, and 32 kHz stimuli (**Fig. 4A**), with ~5-15 dB threshold elevation in the $Cldn9^{+/T}$ mice [F (12, 579) =2.07, P=0.02]. The pattern of hearing threshold remained virtually constant from 2-8 months of monitoring [F (12, 319) =0.50, P=0.91]. Moreover, $Cldn9^{+/+}$ and $Cldn9^{+/T}$mice yielded similar distortion products [F (6, 357) =0.45, P=0.84] (**Fig. 4B**), suggesting normal OHC function. Besides, a significant drop of ABR wave 1 amplitude was observed in the 2 months $Cldn9^{+/T}$ mice comparing to the wild-type littermates (8 kHz F (10, 235)=2.91, P=0.02; 16 kHz F (10, 237)=1.99, P=0.04; 32 kHz F (10, 233)=7.80, P=0.00; click F (10, 233)=3.99, P=0.00 (**S8A-D**). However, wave 1-latency shows no difference between $Cldn9^{+/T}$ and $Cldn9^{+/+}$ mice at 2 months (**S8E-H**). The apparent normal morphology of the ectopic IHCs led to the hypothesis that the IHCs may exhibit functional mechano-electrical transducer (MET) currents. Since active MET channels are partially open at rest, the rapid uptake of the channel permeable lipophilic dye FM1-43 (Gale et al., 2001), was assessed. Results were determined from FM1-43 dye loading of apically located original and ectopic IHCs in 4-week-old $Cldn9^{+/T}$ cochlear site representing ~4-6-kHz characteristic frequencies (CFs). Local perfusion of 10-μM FM1-43 resulted in intense dye labeling at the hair bundle level of original and ectopic IHCs. The dye-membrane partitioning and diffusion across the IHCs' basal aspects occurred within seconds. Z-stacked-time-lapse images were taken below hair bundle level 2-sec post dye exposure and at the basolateral compartment (**Fig. 4C**). The time constants (τ) of dye loading at the bundle and supra-nuclear basal membrane levels for original IHCs were (data from 4 mice); 19.4±1.1 sec (n=27) and 29.0±3.8 sec (n=27), and for ectopic IHCs were 23.1±4.5 sec (n=27) and 47.0±8.4 sec (n=27) (**Fig. 4D**). These results are consistent with functioning IHCs at rest. We conclude that the ectopic IHC bundles are set at the optimum dynamic range to transduce MET current at rest like the original counterparts. IHC MET current magnitudes and kinetic profiles from the original and ectopic rows at the ~3-4-kHz cochlear-place map in P21 mice were comparable, as summarized in **figures 4E-G**. The normalized current-displacement relationships were well-fitted with a two-state Boltzmann function, portraying marked similarities between the original and the ectopic IHC MET currents (**Fig. 4H**). However, the displacement-response relationship for the ectopic IHCs was right-shifted, indicative of reduced sensitivity.

Synaptic features of ectopic IHCs and original IHCs

To determine whether the ectopic IHCs had additional properties in terms of systemic functions, we examined features such as neuronal innervation in both the original and ectopic IHCs. We labeled auditory neurons and IHCs with calretinin (Calb2) antibodies (Sun et al., 2018). Results show Calb2-positive-subtype neurites at the modiolar aspects of both IHCs (**Fig. 5A**). The synapses between the IHCs and auditory neurons at the apical, middle, and basal cochlear locations from 5-week-old $Cldn9^{+/+}$ and $Cldn9^{+/T}$ mice show substantial differences. The organization of afferent synapses was significantly different, identified as paired presynaptic-CtBP2 (red) and postsynaptic-Homer1 (green) immunopuncta. Contrasting $Cldn9^{+/+}$ from $Cldn9^{+/T}$ cochlear samples, results showed reduced synaptic numbers in the $Cldn9^{+/T}$ (**Fig. 5B-C**).

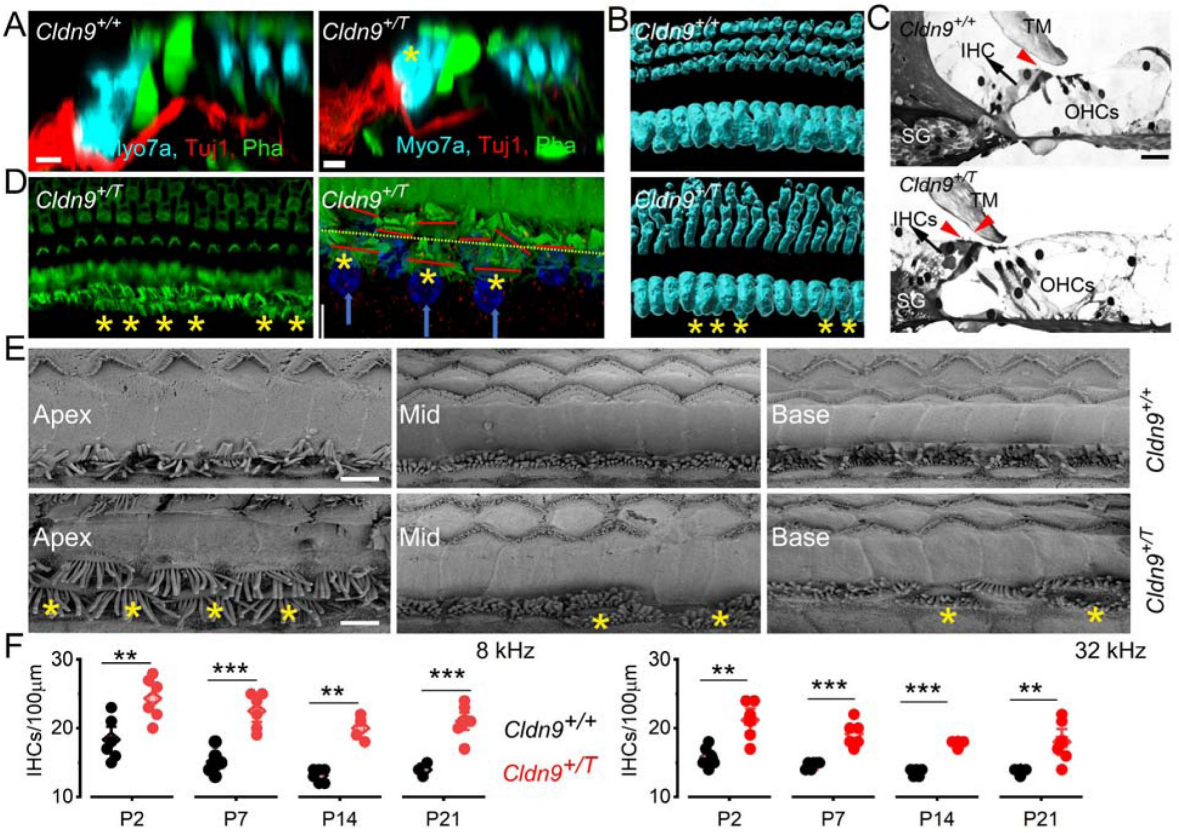

Figure 2.

Cldn9 knockdown-induced supernumerary cochlear IHCs.

A. Radial section of the cochlea partition of 8-wk-old WT (*Cldn9*$^{+/+}$) (left Panel) and *Cldn9*+/T (right Panel) mice. Myosin 7a (cyan) stained IHCs and phalloidin (green) labeled actin stereocilia bundles and other cellular structures, and Tuj1 (red) stained neurons. The yellow asterisks (*) denote ectopic-IHC. Scale bar = 5 μm. **B.** 3-D rendition of cochlear surface preparation (aged 8-wks old), showing a single row of IHCs and three rows of OHCs in the WT (top Panel: *Cldn9*$^{+/+}$) and for the *Cldn9*$^{+/T}$(lower Panel). The ectopic IHCs are marked with (*) Scale bar = 10 μm. **C.** Mid-modiolar section of the 8-week-old cochlea of *Cldn9*$^{+/+}$(top) and *Cldn9*$^{+/T}$ (lower) panels. The red arrows show one and two IHC bundles in the *Cldn9*$^{+/+}$ and *Cldn9*$^{+/T}$cochlear sections, respectively. SG = spiral ganglion, TM= tympanic membrane IHC = inner hair cell, OHCs = outer hair cells Scale bar = 10 μm. **D.** Surface preparation of cochlea of *Cldn9*$^{+/T}$, showing two-rows of IHCs (the 2nd-row IHCs are marked with (*) and higher magnification of a tilted section revealing the nuclei (Dapi stain in blue, and arrow points to the nuclei of the 2nd IHC row). The dotted yellow line shows the hair bundles of the 1st row, and the red lines denote the orientations of the hair bundles. Scale bar = 10 μm. **E.** Scanning electron photomicrographs of the apical (Apex), middle (MT), and basal (Base) cochlear turn of 6-week-old *Cldn9*$^{+/+}$and *Cldn9*$^{+/T}$ mice. The ectopic IHCs are marked with (*). **F.** Summary data of Quantification of IHCs count at 8- and 32-kHz placed cochlear map at postnatal days (P) 2, 7, 14, 21 in *Cldn9*$^{+/+}$compared with *Cldn9*$^{+/T}$ mice. Each data point is the means of 4-blind counts. At 8 kHz cochlear placed-map, the *p* values were P2 = 7.4X10^{-3}, P7 =3.0X10^{-4}, P14 = 2X10^{-3}, and P21 = 1.5X10^{-4}. At 32 kHz cochlear placed-map, the *p* values were P2 = 4.0X10^{-3}, P7 =1.0X10^{-3}, P14 = 8.5X10^{-6}, and P21 = 1.7X10^{-2}.

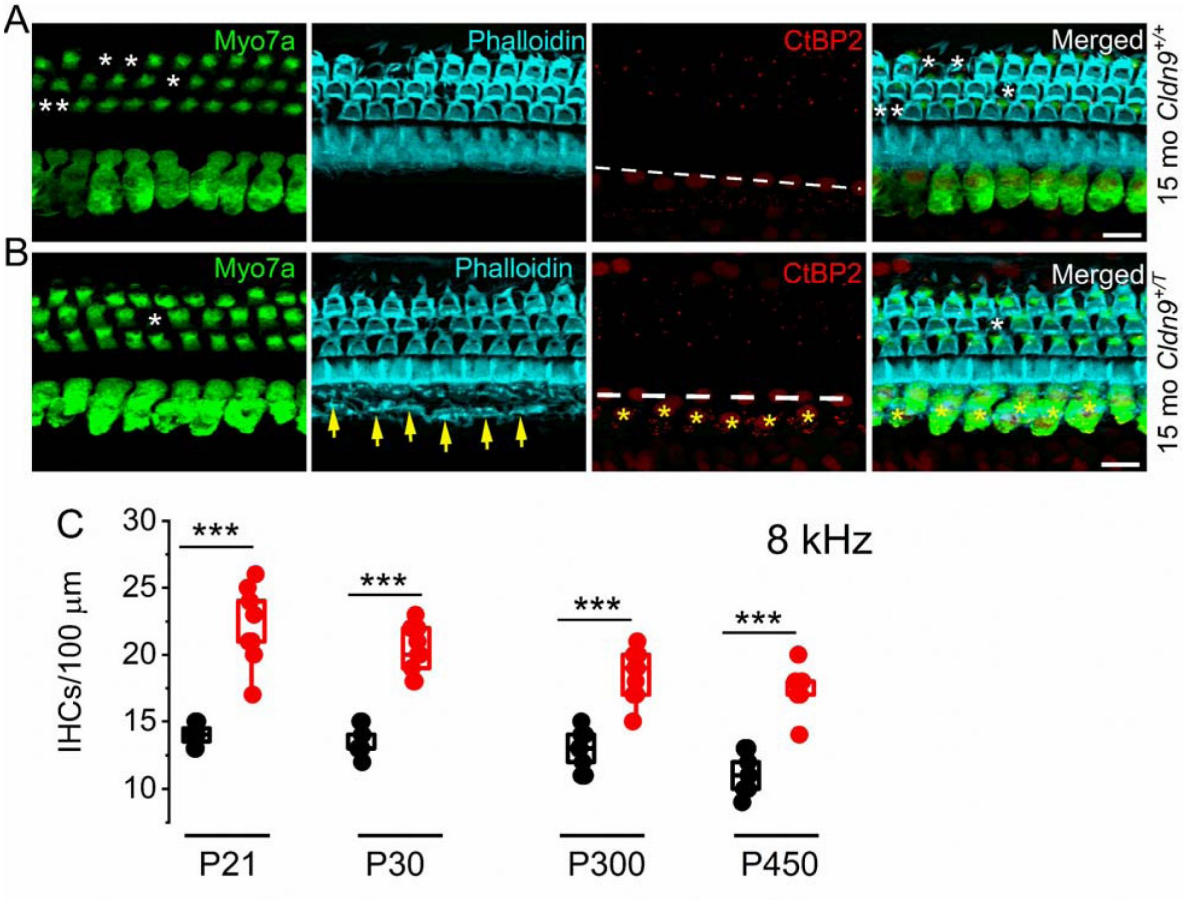

Figure 3.

***Cldn9* knockdown-induced supernumerary IHCs remain intact in older mice.**

A. Surface cochlear preparation of a 15-months (P450) old *Cldn9*$^{+/+}$ mouse shows IHCs and OHCs labeled with Myosin7a (Myo7a) antibody (green) and actin with phalloidin (cyan) and presynaptic maker CtBP2 antibody (red), which is nuclear-positive. The white dash line marks the single row of IHCs. Note that the missing OHCs are marked with white asterisks at 15 months. **B.** Similar preparation as in **A**, from a 15-month-old *Clnd9*$^{+/T}$ mouse. Viable ectopic IHC can be seen with yellow arrows pointing to the hair bundles and nuclei, stained with CtBP2 antibody (*). **C.** Summary data of Quantification of IHCs count at 8- and 32-kHz placed cochlear map at postnatal days (P) 21, 30, 300, and 450 in *Cldn9*$^{+/+}$ compared with *Cldn9*$^{+/T}$mice. Each data point is the mean of 3-blind counts. At 8 kHz cochlear placed-map, the *p* values were P30 = 2.9X10^{-7}, P300 =3.7X10^{-6}, and P450 = 1.4X10^{-7}. At 32 kHz cochlear placed-map, the *p* values were P30 = 1.1X10^{-2}, P300 =4.6X10^{-4}, and P450 = 6.7X10^{-5}.

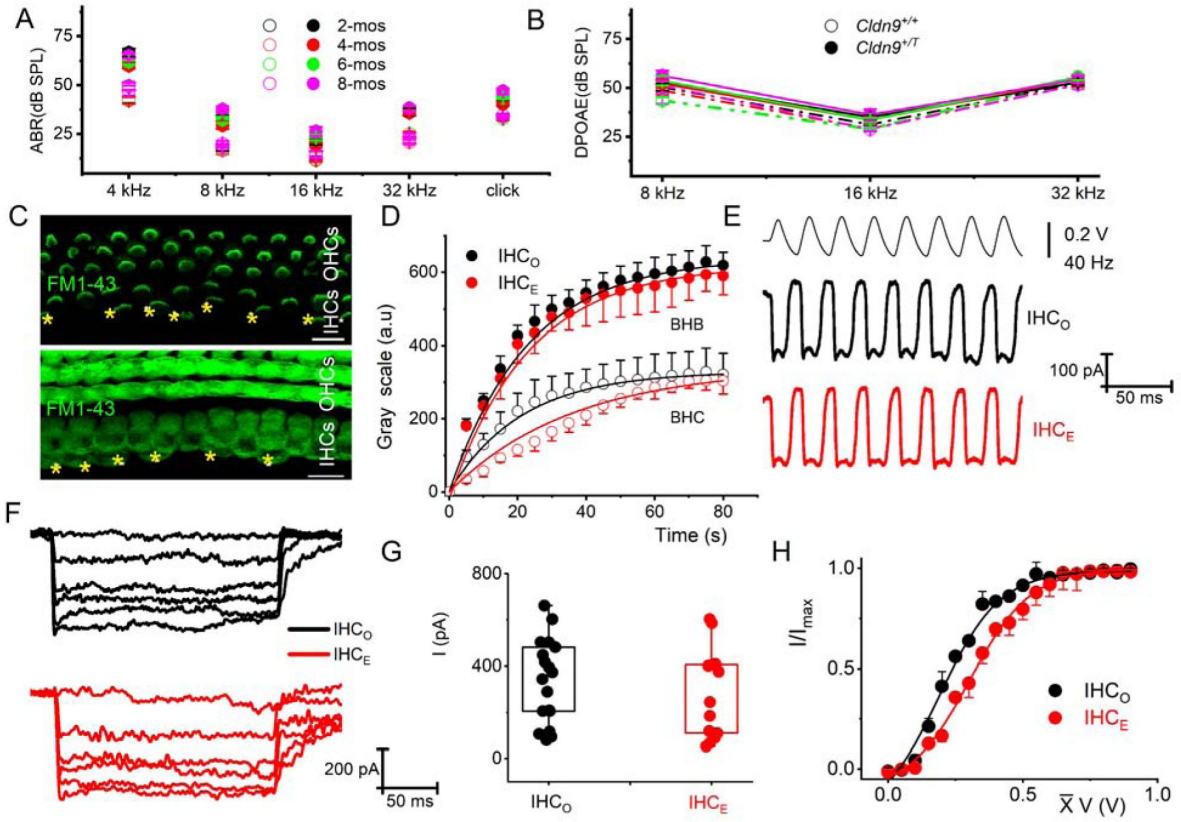

Figure 4.

Auditory brainstem recordings (ABR) and distortion product otoacoustic emissions (DPOAE) assessment and mechanoelectrical transducer channel-FM1-43 permeation and currents elicited from original (O; IHC_O) and ectopic (E; IHC_E) IHC stereocilia bundles.

A, ABR thresholds from the *Cldn9*$^{+/+}$ (open symbols, das lines) and *Cldn9*$^{+/T}$ (solid symbols, solid lines) monitored from 2-8 months. The sound pressure levels (SPL) in dB of pip tones (in kHz) 4, 8, 16, and 32 and broadband clicks delivered to the ear are indicated. ABR thresholds for *Cldn9*$^{+/+}$ (n = 12) and *Cldn9*$^{+/T}$ (n = 17) mice. On average, the *Cldn9*$^{+/T}$ had a 5-15 dB elevated threshold compared to *Cldn9*$^{+/+}$ mice. Within each group of mice, there was no significant shift in ABR threshold from 2-8 months of monitoring. The data means ± SD. **B,** Mean DPOAE threshold for 2-8 months (*Cldn9*$^{+/+}$ group: n=9; *Cldn9*$^{+/T}$ group: n = 14) was tested, measuring the 2f1 - f2 DPOAE over a geometric-mean frequency range at 8, 16, and 32 kHz. The lines and symbols are the same as the labels in **Fig. 4A**. On average, the *Cldn9*$^{+/T}$ had a 5-7 dB elevated threshold compared to *Cldn9*$^{+/+}$ mice. **C,** Fluorescent images of FM1-43 were taken at different time points at two focal planes: the base of IHC bundle (BHB) and the below cuticular plate (BHC) levels of postnatal day (P) 14 *Cldn9*$^{+/T}$cochlea. The ectopic IHC bundles are marked with (*). **D.** Time 0 indicates the onset of dye application (10 mM for the 5-sec duration). Consecutive images at BHB and BHC were taken at 5-s intervals. Dye loaded into this region remained sustained. The dye enters the apical aspects of the cell before being visualized at the basal pole. (Scale bar, 10 μm). The change in fluorescence at focal levels as a function of time (adjusted for the interval between frame capture at each level). Densitometric data of mean pixel intensity were measured in arbitrary grayscale units. Summary data from IHC_O and IHC_E (n = 27 from 3 mice). Frames were taken from 3-4 kHz placed map of the mouse cochlea. The change in fluorescence was fitted with an exponential function, and the time constants (t, in s) of FM1-43 dye loading in IHC_O (in black circles) at BHB and BHC levels,19.4±1.1 (n = 27) and 29.0±3.8 (n = 27). Similar analyses for IHC_E (in red circles) at BHB and BHC levels were 23.1±4.5 (n = 27) and 47.0±8.4 (n = 27). **E,** Typical MET current traces from IHC_O and IHC_E elicited sinusoidal hair bundle deflection at 40 Hz. **F.** MET current elicited a series of ~200-ms hair bundle displacements, using fluid-jet deflection towards the taller stereocilia. Hair cells were held at −80 mV. All recordings were made from apical IHCs. Bundle deflection was elicited with 0.1-0.9 V pressure clamps in 0.1-V steps. Estimates for the exact bundle displacement were not determined. For clarity, a few traces were omitted. **G,** Summary of group data of the maximum IHC MET current measured from IHC_O, 335±181 pA (n = 18) and IHC_E, 268±192 (n = 14) (mean ± SD) **H,** Normalized displacement response relationships fitted with a two-state Boltzmann function. The half-maximum displacement voltage (in V) for IHC_O and IHC_E were 0.20±0.02 and 0.30±0.01 (n= 7).

Moreover, quantifying the mean number of synapses per IHC among the original and ectopic IHCs showed variations along the cochlear axis (**Fig. 5D**). This data suggests that ectopic IHCs are equipped to serve as afferent receptors capable of transducing and transmitting mechanical displacement into neural codes, while synaptic transmission from ectopic IHCs might be compromised because significant differences in synapse numbers were identified.

Postnatal induction of ectopic IHCs by shRNA knockdown

Because pregnant mothers were fed on dox-water from gestation, the ectopic IHCs in *Cldn9*$^{+/T}$ cochlea were of embryonic origin. We designed an efficient shRNA construct to knock down *Cldn9* postnatally. Viral transduction *in vivo*, through round window injection into the cochlear tissue, was monitored with a GFP reporter gene (**Fig. 6A**). We first assessed the efficiency and specificity of the shRNA knockdown of *Cldn9* using quantitative RT-PCR (**S9A**) and immunofluorescence microscopy (**Fig. 6A**). Four days post-injection, there was an ~20-fold reduction in *Cldn9* mRNA relative to nontargeting scrambled shRNA injected cochlea (**Fig. 6A**, **S9**). Transduction *in vivo* of *Cldn9* shRNA into P2-7 inner ears yielded cochleae with ectopic IHCs compared to internal controls, consisting of opposite cochlea injected with nontargeting scrambled shRNA injected, which did not display ectopic IHCs. By contrast, the P14 inner ear injected with *Cldn9*-shRNA produced no detectable increase in ectopic IHCs as counted by three independent blinded observers (**Fig. 6B-D**). Ultrastructural SEM analysis of *Cldn9*-shRNA transduced P2-7 inner ears show ectopic IHC with hair bundles resembling original IHCs (**Fig. 6C**). The MET currents invoked from the ectopic-IHCs induced by postnatal *Cldn9* knockdown were in keeping with functional HCs.

The endocochlear potential and K^+ concentrations in *Cldn9*$^{+/T}$ mice

The cochlear duct is furnished with cellular syncytia, K^+ channels, and transporters/pumps that operate to orchestrate a unidirectional (basal to apical) flux of K^+ at the lateral wall to produce the endocochlear potential (EP, ~+80 mV), an extracellular potential, subserving the proverbial powerhouse for HC functions (Von Bekesy, 1952). A remnant of K^+ flux is a high K^+ endolymph (~140 mM) restricted from leakage into the basolateral aspects of HCs by TJ between HCs and SCs. At four months of age, the magnitude of the EP and the K^+ concentration of the endolymph and perilymph of *Cldn9*$^{+/T}$ mice were variable significantly from age-matched littermates. A slight decline in the amplitude of the EP and a substantial rise in perilymph K^+ was detected in 8-month-old *Cldn9*$^{+/T}$, but there is no statistical difference compared with the detection in 4-month-old Cldn9$^{+/T}$(**S10**). It is unclear whether the modest changes in the EP and K^+ concentration of perilymph can account for the threshold increase in the *Cldn9*$^{+/T}$mice.

Discussions

Fate determination is typically completed by birth in cochlear HCs, the primary receptors for mechanosensory sound detection. Generating functional HCs in the mammalian cochlea, with a proper cellular organization that allows for cochlear sound frequency selectivity, has been a demanding yet unsolved challenge. Consequently, deafness resulting from HC loss, which constitutes a significant portion of sensorineural hearing loss, is incurable. Multiple aspects must be considered in inducing HC differentiation since HCs have distinct functional and structural features along the cochlear axis. For optimal sensing of different sound frequencies, cochlear apical-to-basal HCs have diverse structural configurations and ion channel configurations and densities that sculpt and preserve low-to-high frequency sound processing (Kimitsuki et al., 2001). Additionally, HCs are connected to SCs by TJ proteins, enhancing the sensitivity of cochlear OHC sound amplification and maintaining high K^+ concentration in the endolymph at the apical surface and low K^+ concentration in the perilymph milieu surrounding HCs (Cohen-Salmon

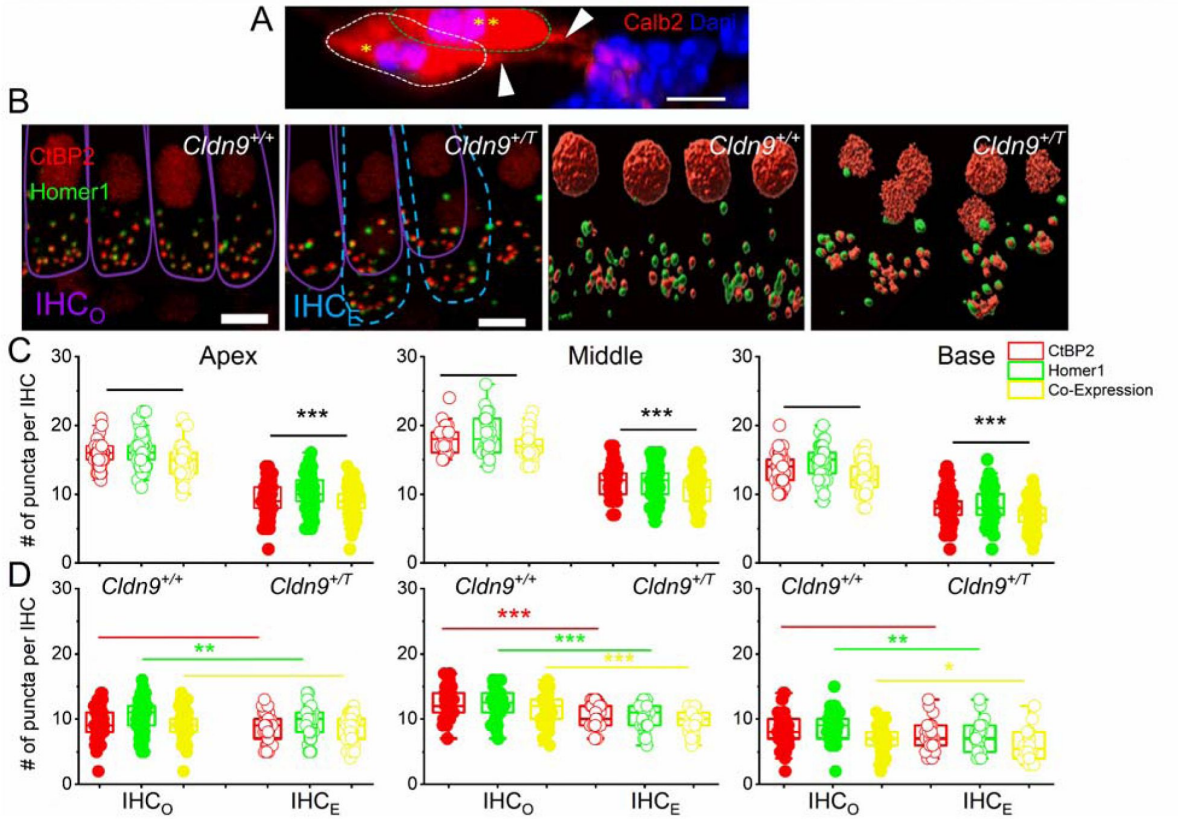

Figure 5.

Pre- and post-synaptic features of original and ectopic IHCs in *Cldn9*$^{+/+}$ and *Cldn9*$^{+/T}$ mice.

A, The innervation of calretinin (Calb2)-positive afferent neurons (red) of an original and ectopic IHCs (marked *, and **) from a 5-wks-old *Cldn9*$^{+/T}$mouse cochlea. Dapi (blue) labeled the nuclei. Arrows point to the nerve terminals. Scale bar = 5 μm. **B,** CtBP2 labeled (red) pre-synapse and Homer1 labeled (green) post-synapse in the cochlear IHCs in the *Cldn9*$^{+/+}$ and *Cldn9*$^{+/T}$ mice. The original IHC (IHC_O) and ectopic IHC (IHC_E) outlines are marked with purple and cyan dashed lines. The two right panels show a 3-D rendition of the pre-and post-synaptic markers in *Cldn9*$^{+/+}$ and *Cldn9*$^{+/T}$ cochleae. Scale bar = 5 μm. **C,** Quantification of the number of pre- (red) and post-synaptic (green) immunopuncta at three tonotopic cochlear locations: apex (3-5 kHz), middle (12-16 kHz), and base (32-40 kHz) from 8-wk-old *Cldn9*$^{+/+}$(open circles) and *Cldn9*$^{+/T}$ (solid circles) mice. Colocalized pre- and post-synaptic marker counts per IHC are shown in yellow. Values (mean ± SD) are illustrated ($p < 0.05$, 0.01, 0.001 = *, **, ***). Comparing pre-, post-synaptic and colocalized markers for apical IHCs, between *Cldn9*$^{+/+}$ (n = 56 from 3 mice) and *Cldn9*$^{+/T}$ (n = 117 from 4 mice) the p values were pre- $p = 2.2X10^{-42}$, post-=$3.5X10^{-30}$, co-expression, $4.3X10^{-34}$. For mid-cochlea IHCs, between *Cldn9*$^{+/+}$(n = 29 from 3 mice) and *Cldn9*$^{+/T}$ (n = 79 from 4 mice) the p values were pre- $p = 1.7X10^{-19}$, post- =$1.3X10^{-14}$, co-expression, $2.5X10^{-18}$. For basal-cochlea IHCs, between *Cldn9*$^{+/+}$(n = 97 from 3 mice) and *Cldn9*$^{+/T}$ (n = 94 from 4 mice) the p values were pre- $p = 3.5X10^{-27}$, post- =$8.2X10^{-27}$, co-expression, $2.9X10^{-26}$. **D,** analysis of synaptic features among IHC_O and IHC_E in *Cldn9*$^{+/T}$ cochlea. At the cochlea apex, comparing pre- post- and colocalized markers between IHC_O (n = 76 from 3 mice) and IHC_E (n = 41 from 3 mice), the p values were pre- $p = 7.0X10^{-2}$, post- = $9.0X10^{-3}$, co-expression = $7.0X10^{-2}$. For mid-cochlea comparing pre-, post- and colocalized markers between IHC_O (n = 48 from 3 mice) and IHC_E (n = 30 from 3 mice) the p values were pre- $p = 1.4X10^{-4}$, post- = $8.9X10^{-5}$, co-expression, $1.7X10^{-5}$. For basal-cochlea comparing pre-, post- and colocalized markers between IHC_O (n = 65 from 3 mice) and IHC_E (n =22 from 3 mice) the p values were pre- $p = 9.0X10^{-2}$, post- = $1.0X10^{-2}$, co-expression, $5.0X10^{-2}$.

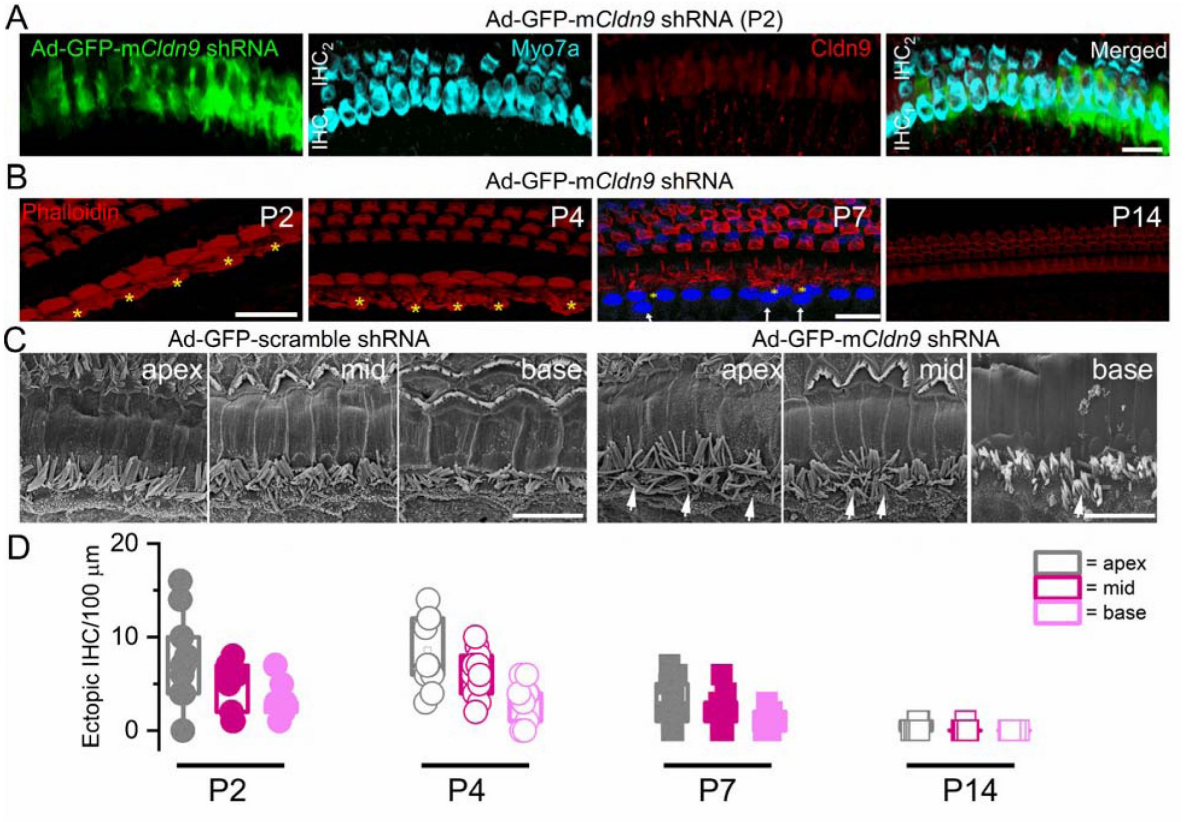

Figure 6.

Postnatal induction of ectopic IHCs with the Cldn9 *shRNA* knockdown

A, Ectopic IHCs observed in P21 cochlea after *Cldn9 shRNA* injection at P2. Downregulation of *Cldn9* levels by ~20-fold compared to scrambled shRNA is shown in **S7A**, and a reduced protein expression (**Fig. 6A**) is shown in the 3rd panel (*Cldn9*, red). GFP (green) expression is a marker for adeno (AD)-virus-transduced cells. The right panel shows the merged image with two rows of IHCs stained with HC marker Myo7a (cyan) and Ad-GFP-mCldn9 shRNA (green) expression in the adjacent row of supporting cells. The Ad-GFP-mCldn9 shRNA (green) is expressed in HCs. **B,** Examples of phalloidin stained whole-mount organ of Corti samples from cochleae of the wild-type mice injected at P2, P4, P7, and P14 with Cldn9 shRNA. The tissues were harvested 20 days after viral injection. Sections at or near the cuticular-plate level show actin labeled with phalloidin (red). Several ectopic IHCs are marked with asterisks in yellow (*). Where nuclei were labeled with Dapi (blue), we marked the ectopic IHC nuclei with a white arrow. **C,** Scanning electron photomicrographs of the apical (apex), middle (mid), and basal (base) cochlear turn of 5-6-wks-old mice after scrambled shRNA and *Cldn9* shRNA injection at P2, showing original and ectopic IHCs (marked with white arrows). Images were captured at the cochlea's apical, middle, and basal contour. **D,** Summary data of quantification of ectopic IHCs count at cochlear apex, middle, and base for samples where *Cldn9* shRNA was injected at P2, P4, P7, and P14. Each data point (n=11) is the mean of 3-blind counts from 3 mice. Ectopic IHCs at-P2 injection (mean/100-mm±SD) for apical, middle, and basal cochlea were 7.5±4.5, 5.0±2.4, and 3.2±1.6; at-P4; 8.5±3.8, 6.1±2.5, and 3.2±1.6; at-P7; 2.8±2.4, 2.4±1.7, and 1.1±1.0; at-P14, 0.2±0.5, 0.1±0.3, and 0.0±0.0. Data are plotted to show individual replicates (n=11; meanIJ±IJSD). There were significant differences at $p<0.05$ level for comparison between P2-7 and P14 F (11,120) = (17) $p = 4.2X10^{-20}$. *Post hoc* comparisons using the Tukey HSD test indicate that post-shRNA injection-induced ectopic IHCs are significantly different at P2 apex vs P14 apex ($p=2.4X10^{-8}$); P2 mid vs. P14 mid ($p=1.3X10^{-4}$); and P2 base vs. P14 base ($p=7.0X10^{-2}$).

et al., 2002). This process establishes a unidirectional K^+ flux in the cochlear duct to generate the EP, which boosts the receptor potential of HC by ~80 mV (Hudspeth, 2008; Von Bekesy, 1952). Thus, besides overcoming the insurmountable terminal differentiation of HCs, newly differentiated HCs *in vivo* should be equipped with features that resemble the original primary HCs to integrate into the specialized cochlear environment.

Among the multiple approaches used with limited success in HC replacement are overexpressing transcription factors involved in prosensory cell differentiation and silencing inhibitory factors in the induction of HC fate. These methods include 1) Transfecting proneural genes, such as *Atoh1*, in embryonic, newborn, and damaged mature cochlear tissue. However, HC-competent cells invariably lose their responsiveness post-birth and in adult animals. In the case of the damaged cochlea, it is challenging to distinguish between transdifferentiated and repaired HCs (Gubbels et al., 2008; Izumikawa et al., 2005; White et al., 2006). 2) Simulating cell division using cell-cycle inhibitors, this strategy activates apoptotic genes, leading to cell death and deafness (Lowenheim et al., 1999). 3) Inhibiting Notch signaling using a γ-secretase inhibitor to stimulate HC differentiation from potential inner ear resident stem cells after noise trauma (Jeon et al., 2011; Mizutari et al., 2013). The scarcity of resident stem cells in adult cochlea may limit this strategy. Thus, multiple therapeutic armamentariums are required to restore hearing in the translational setting.

Previous studies demonstrated that claudin-9 is essential for hearing function and the maintenance of auditory HCs, using an ethyl nitrosourea-induced *Cldn9* mutant mouse model (Nakano et al., 2009), which resulted in OHC degeneration. The current results demonstrate that embryonic regulation of *Cldn9* levels, but not null deletion using the dox-tet-OFF-*Cldn9* transgenic strategy induces functional ectopic IHCs, but not OHCs, along the cochlear contour with increasing numbers from base to apex. These *Cldn9* downregulated-induced IHCs mature, acquiring robust MET currents and neural innervation with synaptic structures markedly like resident IHCs. Results also revealed that postnatal downregulation of *Cldn9* levels *in vivo*, using shRNA, suffice to coordinate SC differentiation into IHCs. Because the ectopic IHCs remain viable for a sizable duration of the mouse's lifespan, the Cldn9 regulatory strategy to induce IHC differentiation subserves a feasible approach to replace lost HCs. The downregulation of Cldn9-mediated selective IHC-increase indicates Cldn9's role during the latter phase of HC differentiation, perhaps post-OHC-fate determination (Garcia-Anoveros et al., 2022). The findings suggest Cldn9-mediated effects may be upstream of the transcriptional factor-mediated trans-differentiation of HCs since the ectopic HCs had features of IHCs, in contrast to primordial HCs generated by *Atoh1* (Yang et al., 2012). It deepens our understanding of the importance of tapping into later stages of HC differentiation, which will likely result in end-organ-specific HCs.

Moreover, a pragmatic strategy requires titrated levels of the TJP to render new HCs without compromising the sensory epithelial cellular syncytial, a decline in the EP, and, significantly, a gradual extracellular K^+ increase that mediates undue HC depolarization and death (Nakano et al., 2009). The critical period at which alteration of TJP level can induce ectopic and new IHCs remains unclear, although, in the current report, we have demonstrated that functional and viable mature ectopic IHCs can be generated by regulating Cldn9 levels.

Our findings that downregulation in the TJP, Cldn9, can regulate IHC differentiation are in conceptual agreement with reports demonstrating that lateral inhibition can affect HC specification (Lanford et al., 1999; Stone and Rubel, 1999). Similar accounts are described where newly formed HCs express delta1-like (DII1) and jagged 2 (Jag2) ligands to mediate Notch1-receptor activation in adjacent antecedent cells, thereby inducing the expression of hairy and enhancer of split (Hes1/5), which suppresses pro-HC transcription factors (Bermingham et al., 1999; Chrysostomou et al., 2012). Consistent with this scheme, interruption of Notch1 signaling during HC development leads to HC overproduction (Brooker et al., 2006; Lanford et al., 1999; Zine et al., 2000). In lateral inhibition, the foremost developing cells adopting HC

fate antagonize the neighboring cells from differentiating into HCs through direct cell-to-cell communication (Brown and Groves, 2020; Mizutari et al., 2013). A possible explanation for the current findings is that TJ proteins, mainly Cldn9, are signaling in Notch-mediated lateral induction (Daudet and Lewis, 2005; Lewis, 1998). Canonical Notch signaling is activated when a Notch ligand, such as Delta-like1 (DI1) in an adjacent HC, binds to a receptor in the SC, resulting in the release of the intracellular domain of the Notch receptor (NICD), which translocate to the nucleus to activate the Notch-targeted gene transcriptions. The findings also confirm that the Notch signaling pathway is responsible for homeostatic TJP expression *in vitro* and promotes barrier function *in vivo* in the RAG1-adoptive transfer model of colitis (Mathern et al., 2014). Indeed, occluding junction depletion disrupts Notch and mitogen-activated protein kinase (MAPK) signaling in intestinal tissue (Fairchild et al., 2016). In the scheme provided in **Figure 7**, Cldn9 may subserve the signaling catalyst to activate NICD cascades that suppress neighboring SCs from trans-differentiation. A limitation of the model is that if *Cldn9*-induced effects were solely dependent on the Notch signaling, ectopic OHCs and IHCs would have ensued. Alternatively, *Cldn9* levels disruption may alter the mechanical properties of the developing and maturing organ of Corti that may trigger ectopic IHC differentiation, an epiphenomenon independent of the Notch signaling. Future studies and emerging findings on HC differentiation will likely address these shortcomings (Kaiser et al., 2022; Li et al., 2023). In cochlear tissue, downregulation of Cldn9 led to concomitant reduced expression of Cldn6 and increased ILDR1. It is unclear whether the induction of ectopic resulted from reduced expression of *Cldn9* alone or combined TJP alterations. It is conceivable that targeting a different TJP may have similar effects on OHC differentiation, requiring impending studies.

Materials and methods

All procedures were performed under research guidelines of the institutional animal care and use committee of the University of Nevada, Reno. Mice of either sex were studied. Doxycycline (dox)-tet-OFF-Cldn9 transgenic mice were generated. In the mouse line, dox concentration can regulate the level of Cldn9 gene expression. The construct consisted of a tetracycline-based genetic switch (tTA cassette) made of three main modules: 1) The tetracycline-controlled transcriptional activator (tTA); 2) The neomycin resistance gene flanked by LoxP sites; and 3) Six copies of the tet operator (tetO) fused to the minimal CMV promoter. The tTA cassette was inserted at the −110 -nucleotide position upstream of the translational start of *Cldn9* to generate the targeting vector. The targeting vector was electroporated into B6 mouse embryonic stem cells. Following the selection in G418, DNA samples from the neomycin-resistant ES cell clones were prepared for short-arm PCR/sequencing analysis and Southern blot analysis to confirm the insertion of the tTA cassette into ES cells. Genetically modified ES cells containing one copy of the tTA cassette were injected into healthy albino B6 blastocysts, and the injected blastocysts were transplanted into the uterus of an albino B6 mouse to generate the chimeric mouse. The chimeric mouse was then bred with albino B6 mice to produce the F1 heterozygous mouse, and the germline transmission was confirmed by tail DNA genotyping. The selection marker was deleted in the tTA cassette by crossing the F1 mouse with the embryonic Cre line (B6.129S4-*Meox2*$^{tm1(cre)Sor}$/J). We backcrossed the B6/129S4 background unto the CBA/CaJ mouse background for 12 generations to prevent the masking of age-related hearing loss effects. 1.0 mg/ml of dox water were fed to *Cldn9* breeding pairs from breeding day one, and heterozygote *(Cldn9*$^{+/T}$*)* and Homozygous (*Cldn9*$^{T/T}$*)* mice and wild-type littermates (*Cldn9*$^{+/+}$*)*, through the time until for the sample collections. The body weights of mice were recorded. Genotyping was performed by PCR using a set of primers that flank the knockin in the *Cldn9* gene: forward primer Cldn9 knockin-F (knockin-sequence): 5'–ATCCACGCTGTTTTGACCTC–3', Cldn9 R3 (Reverse): 5'– TCTGGACCACACAGGACATC– 3'. PCR fragments were separated with 2% agarose gel for an 800 bp product in wild-type, 365 bp in homozygous mutants, and two in heterozygous littermate mice (**Fig. 1**).

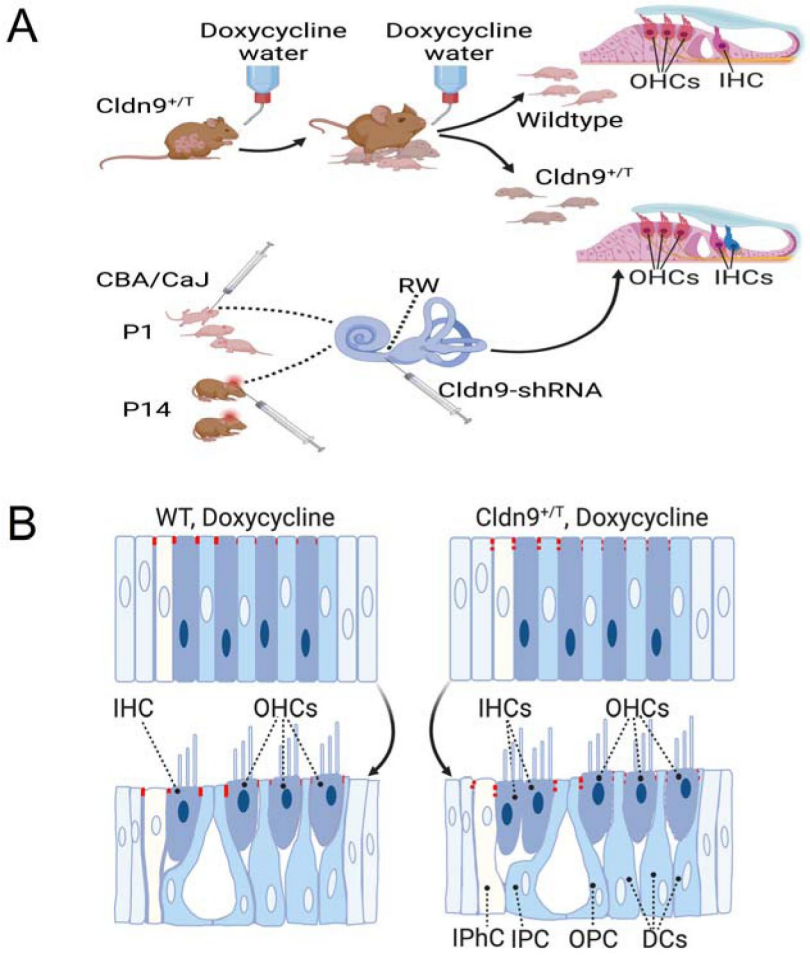

Figure 7.

Study design and summary of findings.

A, The study design schematic included the doxycycline-treated *Cldn9*$^{+/T}$ and *Cldn9*$^{+/+}$mice and postnatal mice transduced with *Cldn9* shRNA. Whereas ectopic IHCs were generated by inner ear injection of Cldn9 shRNA from P2-7, we did not detect significant ectopic IHCs at P14. **B,** The contact lateral inhibition in the late-differentiation stage of IHCs and SCs. The solid red line showed the intact Cldn9 sealing between HCs and SCs, while the dashed red line showed the downregulated *Cldn9* level between cells.

Auditory brainstem recordings (ABR) and Distortion product otoacoustic emissions (DPOAE) measurements

Cldn9 mice (*Cldn9*$^{+/+}$, *Cldn9*$^{+/T}$, and *Cldn9*$^{T/T}$) littermates were tested at 2-8 months of age. Mice were anesthetized with ketamine and xylazine by intraperitoneal (IP) injection (25 mg/kg). Body temperature was monitored using a rectal probe and maintained at 36.8±1.0°C using a homeothermic device (Harvard Apparatus). ABR and DPOAE measurements were described previously (Dou et al., 2004). For ABR assays, thresholds were obtained by presenting tone bursts at 4, 8, 16, and 32 kHz and a clicking sound from 0 dB to 90 dB sound pressure levels (SPL) in 5 dB intervals. Tones were 2.5 ms, while click was 0.1 ms in duration, with a repetition rate of 21/s. Electrodes were placed sub-dermally behind the tested ear (reference), the vertex (active), and the back (ground). Evoked potentials were averaged over 512 repetitions and collected using a Tucker Davis Technology (TDT) RZ6 processor and BioSigRZ software. The threshold was defined as the lowest intensity of stimulation that yielded a repeatable waveform based on an identifiable ABR wave.

DPOAE measurements were performed using the same TDT system with two calibrated MF1 speakers connected to an ER10B+ microphone. Data was collected every 21 ms and averaged 512 times. DPOAEs were recorded using two pure tones with frequencies f1 and f2, using an f2/f1 ratio of 1.2. Input/output (I/O) functions were obtained by increasing the primary tone L1 (and corresponding L2) in 5-dB steps from 20 to 80 dB SPL at 8, 16, and 32 kHz frequencies. During DPOAE testing, the probe assembly was placed in the mouse's left ear canal after visual inspection to ensure no ear infection or inflammation of the tympanic membrane. DPOAE thresholds were defined as the lowest level of f1 required to produce a DPOAE ≥ −5 dB SPL(Chen et al., 2021).

Cochlear mapping and hair cells and synaptic counts

The cochlea was micro-dissected into three to five pieces following the method described (Montgomery and Cox, 2016). Cochlear pieces were measured, and a frequency map was computed based on a 3D reconstruction of the sensory epithelium for HCs and synapse count of associated structures to relevant frequency regions using a custom plug-in to ImageJ (Muniak et al., 2013). Confocal z-stacks of the 4, 8, 16, and 32 kHz areas were collected using a Leica Stellaris8 (Leica) and Nikon A1R laser scanning confocal microscope (Nikon Instruments Inc.). Images were gathered in a 512 x 512 raster using a high-resolution oil immersion objective (60x). IHCs and OHCs at the frequency locations were quantified using myosin-VIIa-positive as an HC-marker within a 70-100-μm field (Chen et al., 2021). Synaptic ribbons and homer-labeled puncta could be counted manually or automatically by setting the filters for the spots function using 3D (x-y-z axis) representations of each confocal z-stack with the microscopic image analysis software Imaris (Oxford Instruments, USA).

Inner ear histological analysis

The cochleae were intra-labyrinthine perfused through the oval and round windows with 4% paraformaldehyde (PFA). The samples were decalcified in 10% EDTA up to 72-96 hrs, depending on the age, at 4°C. Micro dissected pieces were immunostained with antibodies to the following: (1) mouse anti-C-terminal binding protein 2 (pre-synaptic-marker, BD Biosciences, 1:200, Cat # 612044), (2) rabbit anti-myosin-VIIa (HC-marker, Proteus Biosciences, Inc,1:600, Cat # 25-6790), (3) mouse anti-sox2 (supporting cell (SC)-marker, Santa Cruz Biotechnology, Inc, 1:200, Cat # sc-365823), and (4) rabbit anti-Homer 1 (post-synaptic marker, Synaptic Systems, 1:250, Cat # 160 003), (5) rabbit anti-immunoglobulin like domain containing receptor 1 (ILDR1) (*Antibodies-online.com*, 1:200, Cat # ABIN1386369), (6) mouse anti-Cldn9 (Santa Cruz, 1:200, Cat # sc-398836), (7) mouse anti-Cldn6 (Santa Cruz, 1:200, Cat # sc-393671), (8) rabbit anti-Sox2 (Abcam, 1:200, Cat # ab97959), (9) rabbit anti-Tuj1 and chicken anti-Tuj1 (Abcam,1:500, Cat # ab18207, ab41489), (10) goat anti-calretinin (Swant Inc., 1:500, code # CG1), (11) mouse anti-calretinin (Millipore Sigma,

1:200, Cat # MAB1568), (12) rabbit anti-Prestin (Santa Cruz, 1:200, Cat # sc-22692), and (13) rabbit anti-calbindin (Cell signaling technology, 1:200, Cat # 13176S) with appropriate secondary antibodies coupled to Alexa-405, −488, −568, and −647 fluorophores.. DAPI labeled the cell nucleus after secondary antibody incubation. Samples were stained with phalloidin and mounted with Fluoro-Gel (Electron Microscopy Sciences). Images were captured with a confocal microscope.

RNA extraction and quantitative RT-PCR of Cochlear tissue

The cochlea was dissected from the mouse and homogenized on ice. Because of limited tissue, we combined 10-15 mice cochleae for the study. Total RNA was isolated using the RNeasy Plus Mini Kit (Qiagen), and cDNA was generated using the RT2 First Strand Kit (Qiagen). cDNA was combined with RT2 SYBR Green Master Mix (Qiagen), specific qRT-PCR primers, and qRT-PCR analysis was run using the ViiaTM 7 Real-Time PCR System (ABI). Primer efficiencies were determined by standard dilution curve analysis. Three separate samples were used from 10 animals for each group. The experiments from each sample were performed in triplicate, and average cycle threshold (Ct) values were normalized to GAPDH expression. ΔΔCt values were determined relative to *Cldn9*$^{+/+}$ cochlear samples. Fold change was defined as 2(−ΔΔCt). Primers used include Gapdh (SA Biosciences) and Cldn9 (ThermoFisher).

Electron Microscopy

Transmission electron microscopy (TEM) and scanning electron microscopy (SEM) of cochlear sensory epithelia were performed as described (Schwander et al., 2007; Senften et al., 2006). Five to eight-week-old *Cldn9* mice and littermates were sacrificed for TEM, and the cochleae were fixed in 2.5% glutaraldehyde in 0.1 M cacodylate buffer at 4°C overnight. After several washes with buffer alone, cochleae were fixed in 1% osmium tetroxide at RT for 1-hr. After that, the fixed cochleae were decalcified in 10% EDTA for 3–4 days. Fixed and decalcified cochleae were dehydrated using a graded ethanol series and embedded in epoxy resin. Ultrathin sections were cut with a diamond knife. Specimens were examined using an electron microscope.

For SEM, mice were perfused with 4% PFA in 1x PBS, inner ears were isolated, and the stapes footplate was removed. Ears were flushed and fixed overnight in 4% PFA and 2.5% glutaraldehyde in 1x PBS. After washing in ddH_2O 3X for 1 hour, the samples were post-fixed with 1% osmium tetroxide for approximately 1 hour. Samples were washed before decalcifying for 3-4 days in 0.25 M EDTA at 4°C with daily solution changes. The cochleae were micro dissected, the tectorial membranes removed, and gradually dehydrated in 30%, 50%, 70%, 80%, 90%, 100% ethanol, 2:1 ethanol/hexamethyldisilazane (HMDS, Thermo Scientific #A15139.AE), 1:2 ethanol/HMDS, and finally 100% HMDS. Samples were transferred to an open well plate in HMDS and allowed to air dry overnight in a fume hood. They were then mounted on aluminum stubs (Ted Pella #16111) using double-sided carbon tape (EMS #77817-12) and stored in a specimen mount holder (EMS #76510) sealed in a desiccator until sputter-coated with Au/Pd (Emitech Sputter Coater K550) and viewed. Images were captured utilizing the Hitachi S-4800 SEM. An accelerating voltage of 1kV and 5kV was used. Images were compiled using CorelDRAW X7 graphic suite software.

Measurements of the endocochlear potential (EP) and K^+ concentration

Cldn9 heterozygote mice and wild-type littermates were anesthetized using ketamine and xylazine (100/25 mg/kg, i.p.) and K^+ concentration, and the EP was measured using double-barreled microelectrodes. An incision was made along the midline of the neck, and soft tissues were bluntly dissected laterally to expose the trachea and the animal's left bulla. A tracheostomy was done, and the musculature over the bulla was cut posteriorly to expose the bone. A small hole was made in the cochlear capsule directly over the scala media of the lower basal turn. The EP electrode was filled with 300 mM NaCl, the K^+-selective barrel was silanized, and the tip was filled with a liquid ion exchange (Fluka 60398, K^+ ionophore I-Cocktail B) that was backfilled with 150 mM KCl. A

round-window approach made measurements in the basal turn of the cochlea through the basilar membrane of the first turn. The K^+-selective electrode was calibrated in solutions with known cation (K^+ and Na^+) concentrations *in situ* at 37°C.

shRNA CLDN9 knockdown

siRNAs were designed, using siRNA at WHITEHEAD software, and cloned under U6 promoter in pSilencer5.1-U6 vector to produce hairpin siRNAs (shRNAs; Vector Biolabs, NM_020293). shRNA was packaged into adeno-associated virus constructs: AAV/Anc80L65-GFP-U6-mCLDN9-shRNA (4) at $1.0X10^{12}$ GC/mL titer. shRNA sequence for mouse CLDN9 is 5'-CACC GTGCTTCGGGACTGGATAAGACTCGAGTCTTATCCAGTCCCGAAGCAC TTTTT-3'. 1.0 µl shRNA or scrambled shRNA was injected into the round window of mice at P2 – 7 and P14. Mice were anesthetized by induced hypothermia and kept on a cold surface during the injection procedure. After disinfecting the skin with 70% ethanol and Povidone iodine, an incision was made in only the left ear (experiment) and right ear (scramble shRNA injection). Underlying fat and soft tissue were carefully dissected to expose the round window of the cochlea. The glass pipette was pulled with a P-2000 (Sutter Instrument, Novato, CA) and sharpened with a BV-10 Micropipette Beveler (Sutter Instrument, Novato, CA). The shRNA was injected using a nanoinjector (Sutter Instrument, Novato, CA). After all the shRNA was injected into the round window, the pipette was left in place for 30 seconds before removal. The muscles and fat tissue were covered, and the skin was closed with a polypropylene suture. The mice were kept on the warm bedding heated by a heating pad for recovery before returning to their mother. Total surgery time did not exceed 15 min.

Voltage-clamp recording of hair cell mechanoelectrical transducer (MET) current

Patch-clamp experiments were performed in the standard whole-cell mode using an Axopatch 200B amplifier (Axon Instruments). Patch electrodes were pulled with a horizontal puller (Sutter Ins. Navato, CA) and had a resistance of 2–3 MΩ when filled with pipette solution consisting of (in mM) 135 CsCl, 10 HEPES, 2.5 EGTA, 0.25 $CaCl_2$, $MgCl_2$, 4 MgATP, and 0.4 Na_2GTP (pH adjusted to 7.3 with CsOH). The bath solution consisted of (in mM) 130 NaCl, 3 KCl, 1 $MgCl_2$, 10 HEPES, 2.5 $CaCl_2$, and 10 glucose (pH was adjusted to 7.3 using NaOH). Currents were sampled at 20 kHz and filtered at 2 kHz. Voltages were not corrected for a liquid junction potential. No leak current subtraction was performed. Cells were held at −80 mV. All electrophysiological experiments were performed at RT (21-22°C). We used stepwise and sinewave mechanical stimulation of IHC bundles through a piezo-driven fluid-jet stimulator to record IHC mechanoelectrical transducer (MET) currents. We represented the bundle displacement in the form of applied piezo-driven voltage. Bundle displacement was not calibrated for each cell because of variations in stimulating probe positions relative to the stimulated hair bundle.

Data analysis

The ABR and DPOAE data were analyzed using GraphPad Prism 7 (GraphPad Software, San Diego, CA, US) and OriginPro 2020 (OriginLab Corp., Northampton, Mass, US). Three-way ANOVA was used to analyze the ABR and DPOAE threshold. Two-way ANOVA was applied for the ABR wave 1 amplitude/latency data, synapse count, and HCs count. Significance was assumed at a *p*-value of 0.05 in all statistical analyses.

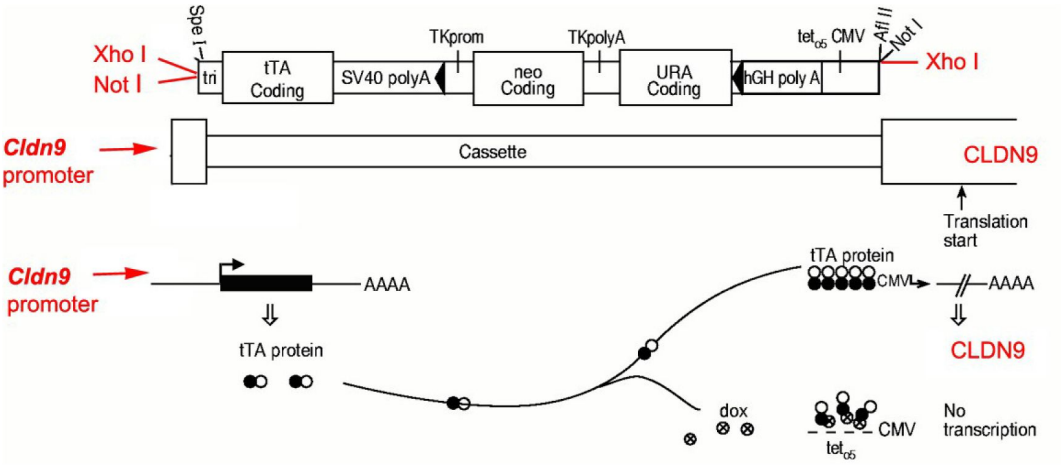

Supplement S1

Schematic diagram of the construct used to regulate translation of CLDN9.

We will use the tTA ("tet-off") cassette developed by Seeburg and Adelman for expressing the SK3 channel {Bond, 2000 #182} (Bond et al., 2000) and modified to include unique *Not* I and *Xho* I cloning sites at each end of the cassette. The cassette contains three motifs: i.) tTA preceded by the tri-partite leader sequence that confers highly efficient translational initiation followed by the SV40 polyA and transcriptional termination sequence, ii.) bacterial neomycin (G418) resistance gene driven by the herpes simplex virus thymidine kinase (TK) promoter and the yeast URA3 gene; these selectable markers are flanked by loxP sites and followed by the human growth hormone (hGH) polyA and transcriptional termination sequence, iii.) six copies of the tet operator (tetO6) fused to the minimal cytomegalovirus (CMV) promoter. The native *Cldn9* promoter drives the expression of tTA, which in CLDN9 from the tetO6/CMV promoter. In the presence of Dox (crossed circles), tTA is bound and cannot bind to the tetO6/CMV promoter, thereby turning off the transcription of CLDN9.

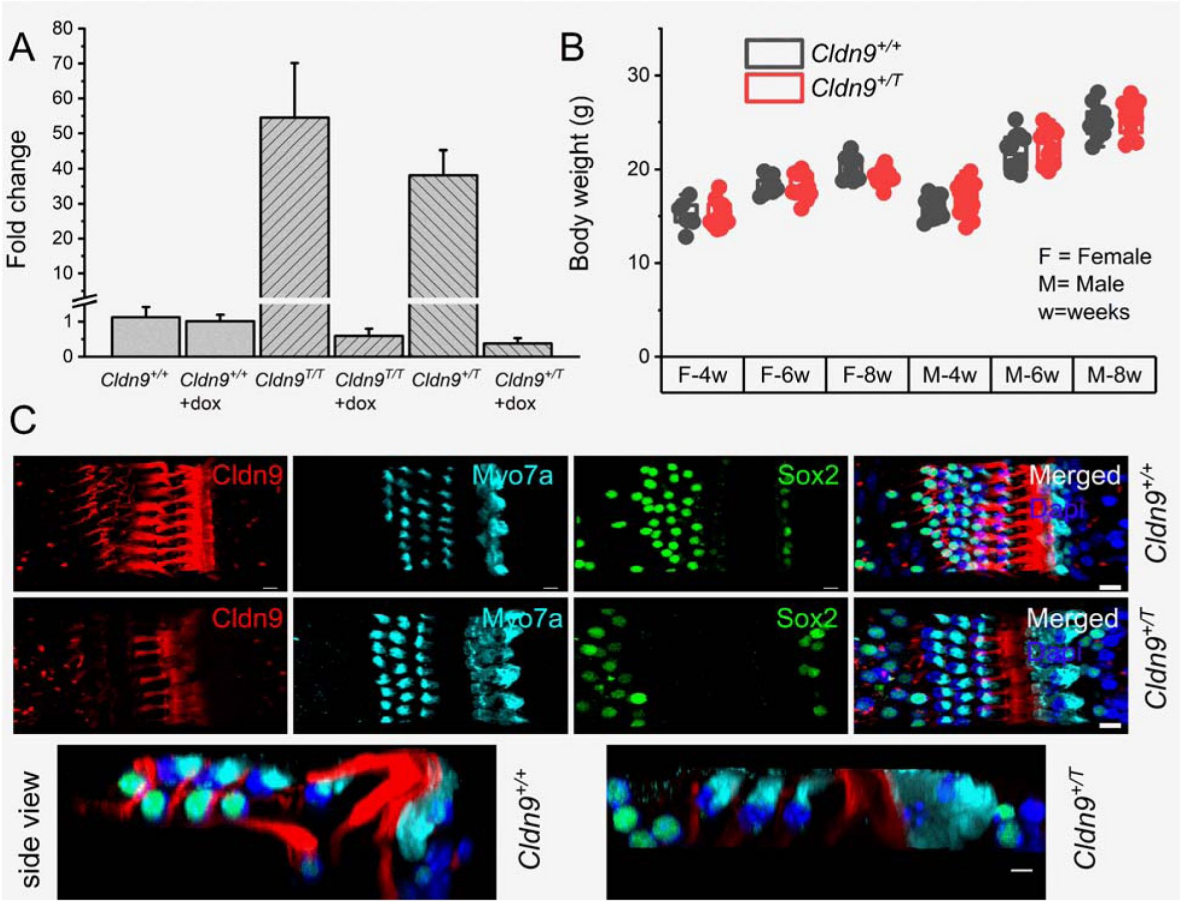

S2

A. Quantitative RT-PCR of *Cldn9* transcripts from cochlear tissue from six groups of animals, including $Cldn9^{T/T}$, $Cldn9^{+/T}$ with and without dox treatment compared with WT littermates with and without dox treatment. **B.** Body weight measurements of female and male mice from dox-treated $Cldn9^{+/T}$ and $Cldn9^{+/+}$ groups were recorded at 4, 6, and 8 wks old. **C.** The immunostaining of *Cldn9* in 8-wk old WT ($Cldn9^{+/+}$) mouse cochlea*Cldn9* (red), IHC stained myosin7a (cyan) and supporting cells stained Sox2 (green) and Dapi (blue) for nuclear stain. Scale = 10 μm.

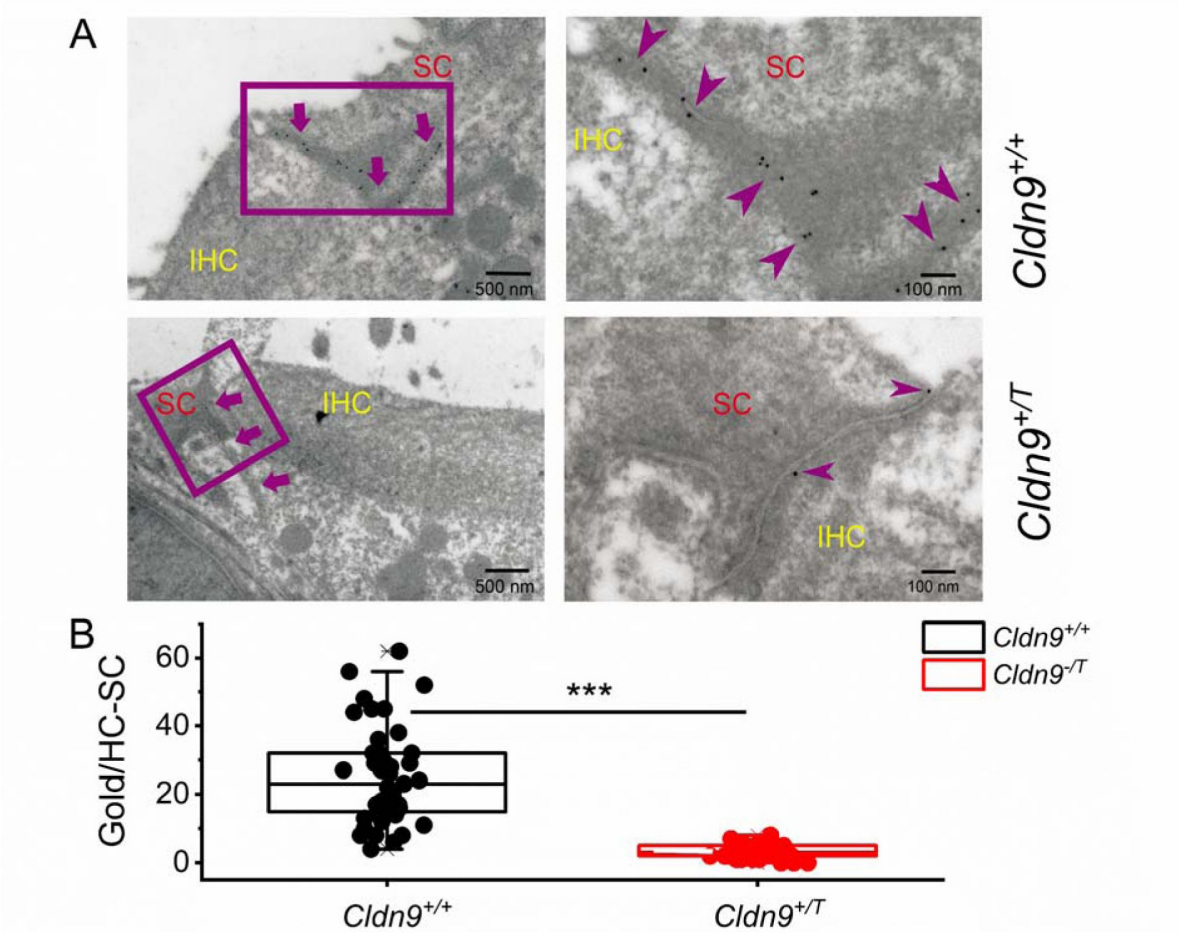

S3

Immunogold localization of Cldn9 in *Cldn9$^{+/T}$* and *Cldn9$^{+/+}$* mice.

A. Cldn9 expression sites between inner hair cells (IHCs) and supporting cells (SCs) were examined with immunogold electron microscopy with the post-embedding technique. Secondary antibodies are conjugated to 16-nm colloidal gold particles (arrows). Gold particles were noted at the junctions between SC and IHCs in *Cldn9$^{+/+}$* mice cochlea (indicated). *Cldn9$^{+/T}$* mice had reduced gold particles. **B.** Summary of gold particle counts between IHC and SC between Cldn9$^{+/+}$ and Cldn9$^{+/T}$. Mean gold particles (mean±SD) for *Cldn9$^{+/+}$*= 25±14 (n = 41 from 3 cochleae) and for *Cldn9$^{+/T}$* = 3±2 (n = 41, from 4 cochleae), $p = 2.8X10^{-15}$.

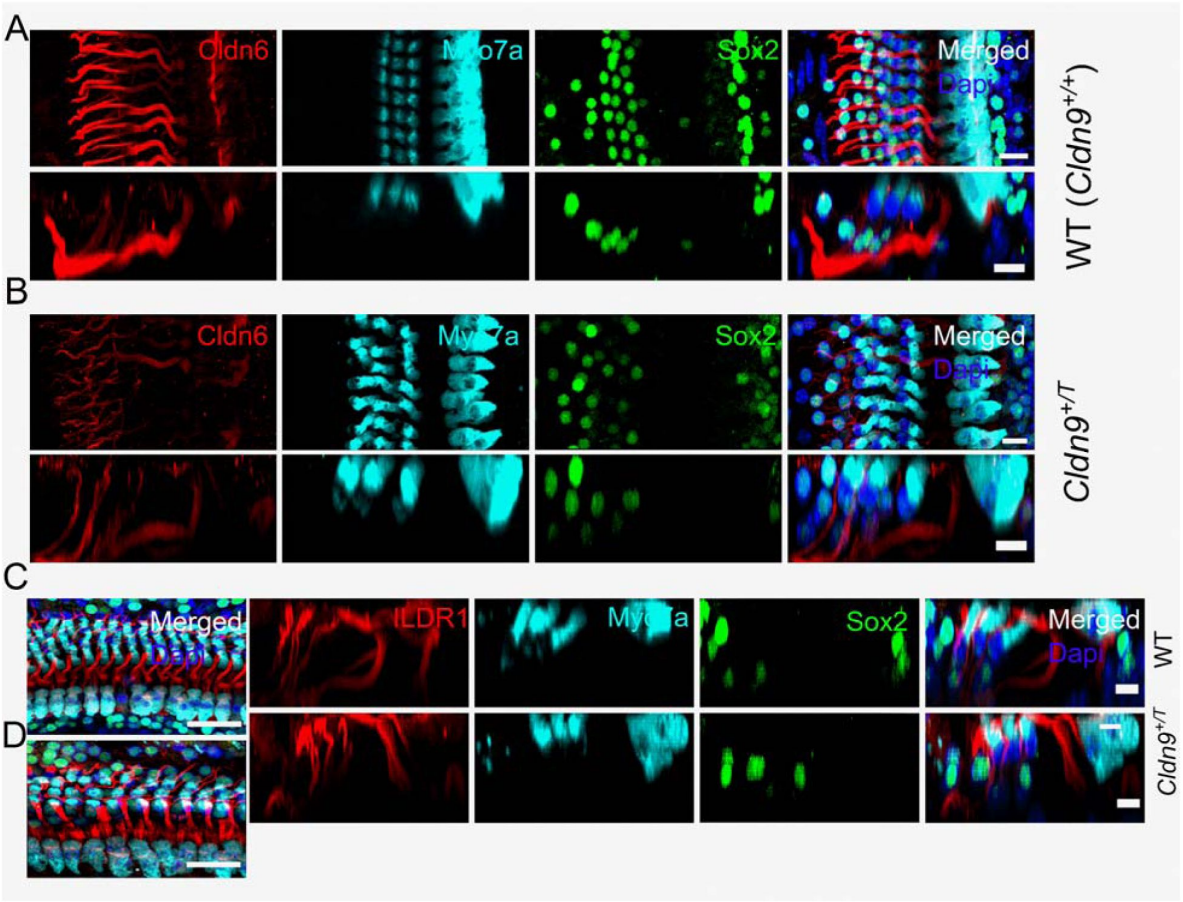

S4

The expression of cldn6 and ILDR1 in the organ of Corti.

A-B, The immunostaining of Cldn6 (red) in the mouse cochlea from *Cldn9*$^{+/+}$ (wildtype, WT) and C*ldn9*$^{+/T}$. The lower Panel is the side view of the cochlear section. HCs were labeled with Myo7a (cyan) supporting cells with Sox2 (green) and Dapi-stained (blue) nuclei. The levels of Cldn6 were reduced in the *Cldn9*$^{+/T}$ cochlea. **C-D**, The immunostaining of ILDR1 (red) in the mouse cochlea from *Cldn9*$^{+/+}$ and C*ldn9*$^{+/T}$. The lower Panel is the side view of the cochlear section. HCs were labeled with Myo7a (cyan) supporting cells with Sox2 (green) and Dapi-stained (blue) nuclei. The levels of ILDR1 were increased in the *Cldn9*$^{+/T}$ cochlea. Scale bar = 10 μm.

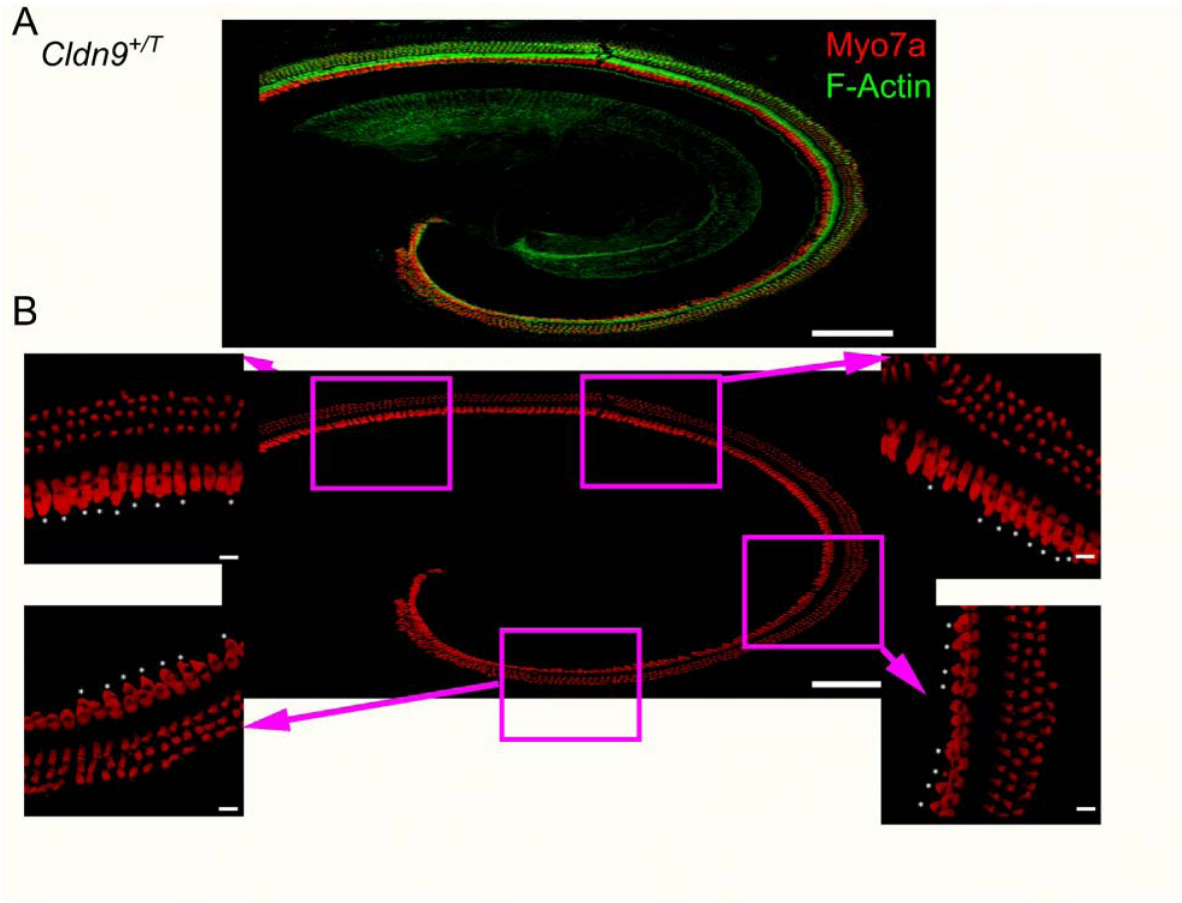

S5

The ectopic HCs can be seen along the cochlear apicobasal contour.

A, The immunostaining of Myosin 7a (red) and F-actin (green) in C*ldn9*$^{+/T}$ mouse cochlear apical segment. **B**, Panel shows smaller segments magnified to clarify and detect multiple ectopic HCs. HCs were labeled with Myo7a (red). Scale bar = 10 μm.

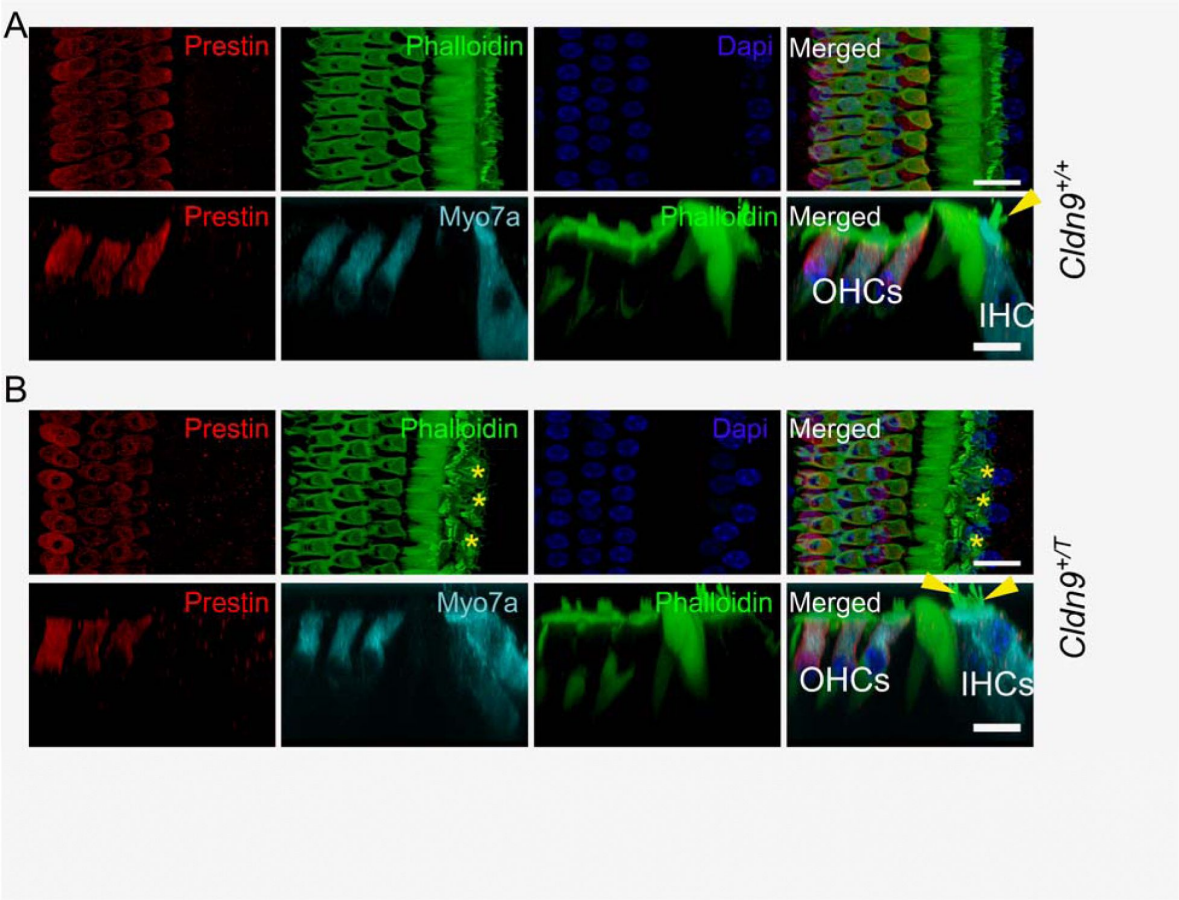

S6

The ectopic HCs stain positively to Myosin 7a but negatively to prestin antibodies

A-B, The immunostaining of prestin (red) in the mouse cochlea from *Cldn9*$^{+/+}$ (wildtype, WT) and *Cldn9*$^{+/T}$. The lower Panel is the side view of the cochlear section. HCs were labeled with Myo7a (cyan) phalloidin-stained actin (green) and Dapi-stained (blue) nuclei. Scale bar = 10 μm.

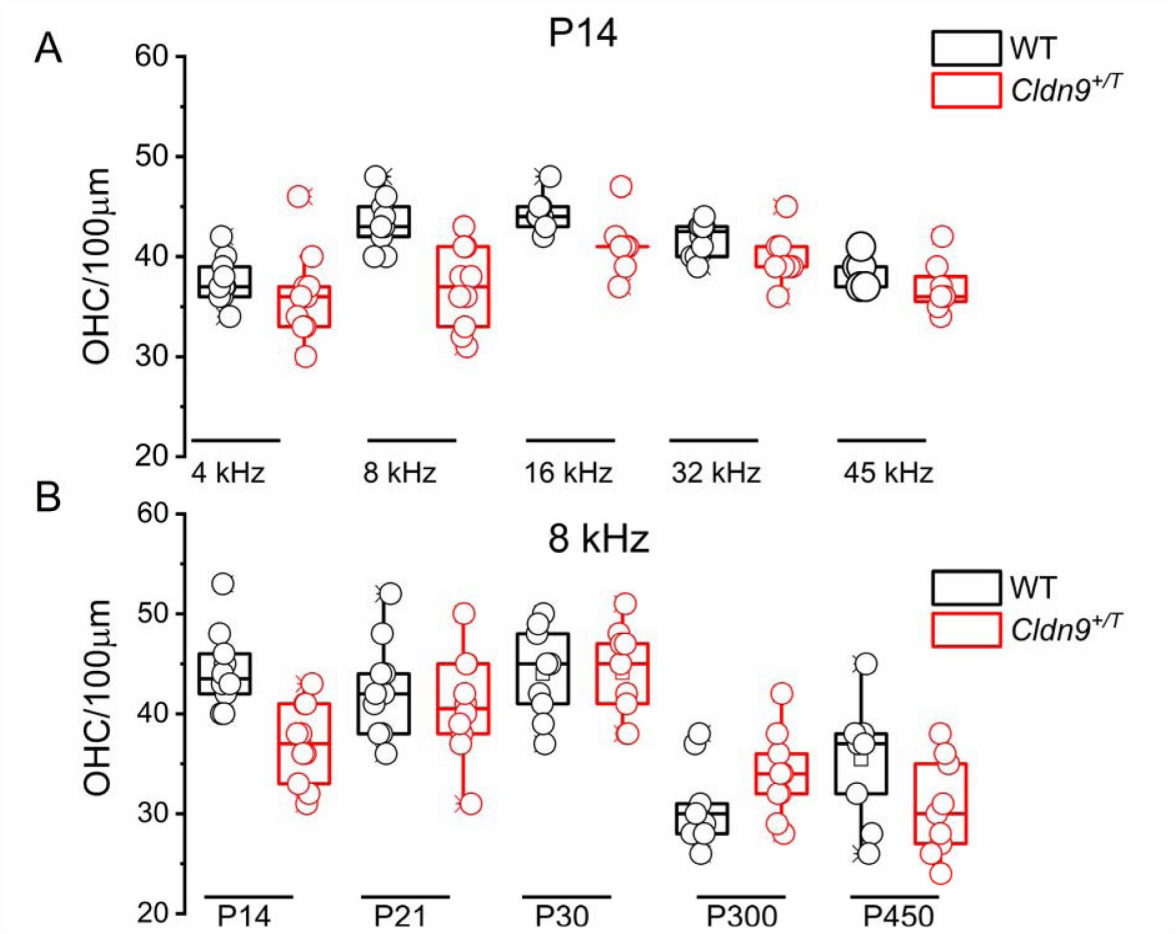

S7

A. Summary data of Quantification of OHCs count at ~4, 8, 16, 32, and 45-kHz placed cochlear map at postnatal days (P14) in *Cldn9*$^{+/+}$(WT, in black symbols) compared with *Cldn9*$^{+/T}$ (in red symbols) mice. Each data point is the mean of 4-blind counts. **B.** At 8 kHz cochlear placed-map, OHC counts were changed for P14, 21, 30, 300, and 450 mice. OHC numbers remained relatively constant (P14-30) until P300-450) when they were reduced.

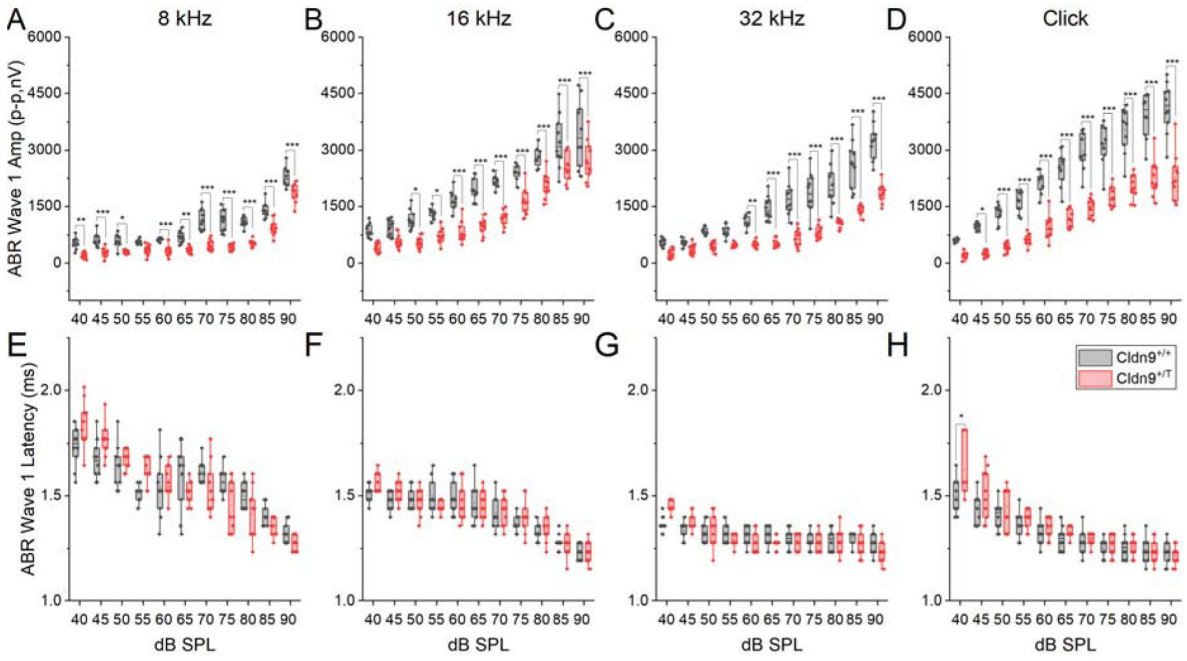

S8

The ABR wave one amplitude and latency in *Cldn9*$^{+/T}$ and *Cldn9*$^{+/+}$ mice.

A-D. ABR wave 1 amplitude was decreased, while the latency varied in *Cldn9*$^{+/T}$ mice compared to *Cldn9*$^{+/+}$ mice when measured at 8 kHz, 16 kHz, 32 kHz, and click **(E-H).** * P < 0.05, ** P < 0.01, *** P < 0.001.

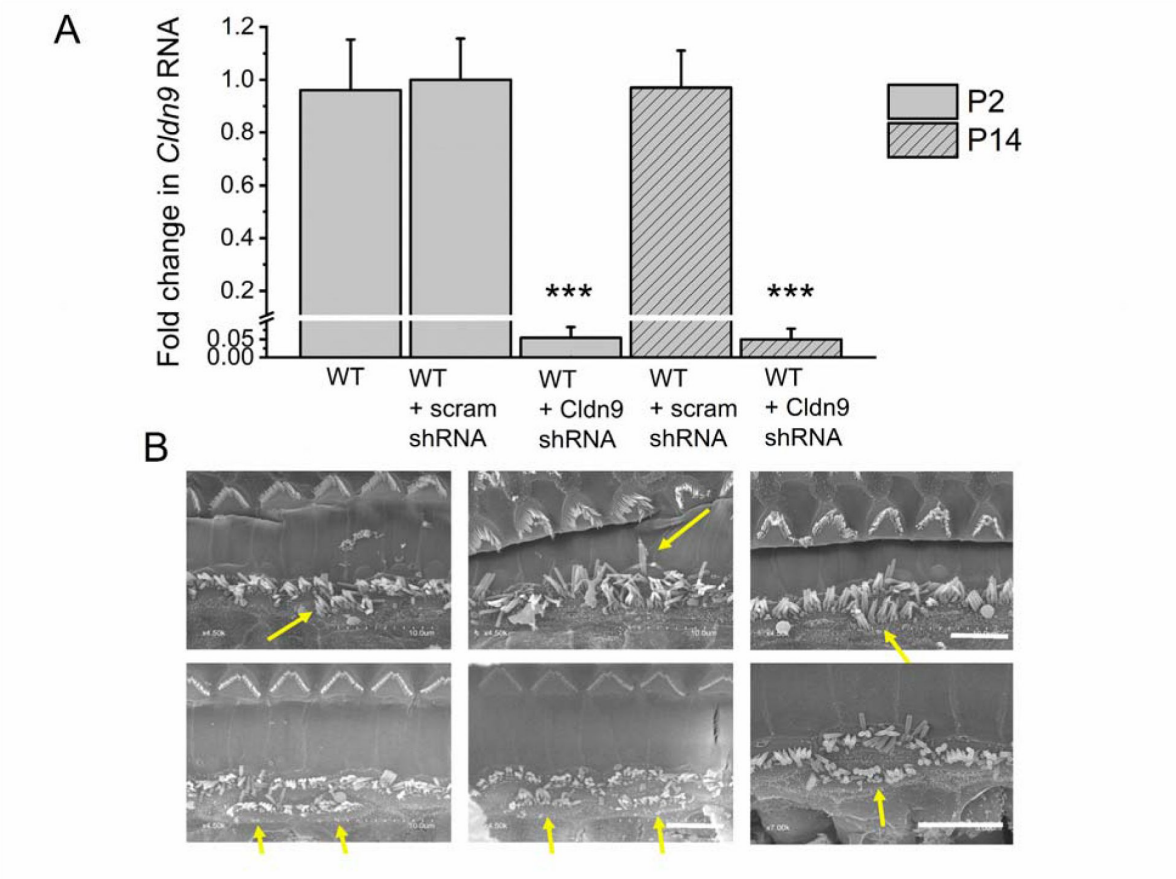

S9

A. Quantitative RT-PCR of *Cldn9* transcripts from cochlear tissue from WT un-injected, scrambled (scram), and shRNA P2- and P14-old-injected mice. **B.** Examples of SEM of the shRNA-injected cochlea (age of samples at the harvesting time (P24) for imaging and the age at shCldn9 injection P2). Yellow arrows show ectopic IHC bundles.

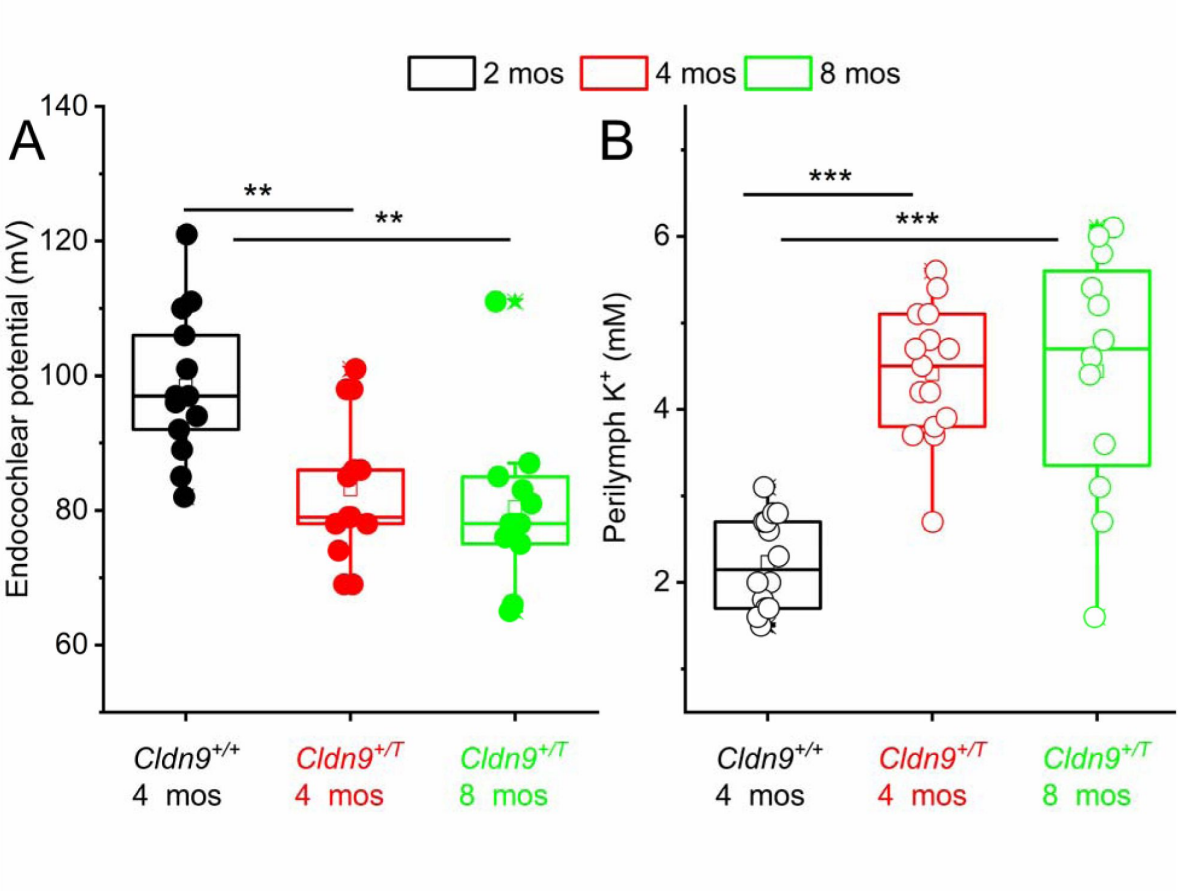

S10

The endocochlear potential (EP) and perilymph K^+ in *Cldn9*$^{+/+}$ and *Cldn9*$^{+/T}$mice.

A. Measurement of the EP at the basal turn of the cochlea, in 4-month-old *Cldn9*$^{+/+}$ = 99±11 mV (n=13), *Cldn9*$^{+/T}$ = 83±11 mV (n=13) and at 8-month-old for *Cldn9*$^{+/T}$ = 80±12 (mV) (n=11). There were significant differences at $p<0.05$ level for comparison between *Cldn9*$^{+/+}$ vs. *Cldn9*$^{+/T}$F(2,34)=(9.3) $p = 5.9X10^{-4}$. *Post hoc* comparisons using the Tukey HSD test indicate *Cldn9*$^{+/+}$ vs. *Cldn9*$^{+/T}$ at 4 months (p=4.0X10^{-3}); *Cldn9*$^{+/+}$ (4 months) vs. *Cldn9*$^{+/T}$ (8 months) (p=1.2X10^{-3}); are significantly different. **B.** Recordings of perilymph K^+, in 4-month-old *Cldn9*$^{+/+}$ = 2.2±0.5 mM (n=14), *Cldn9*$^{+/T}$ = 4.4±0.8 mM (n=15) and at 8-month-old for *Cldn9*$^{+/T}$= 4.4±1.4 (mM) (n=12). There were significant differences at $p<0.05$ level for comparison between *Cldn9*$^{+/+}$ vs. *Cldn9*$^{+/T}$ F (2,36)=(24.4) $p = 1.6X10^{-7}$. *Post hoc* comparisons using the Tukey HSD test indicate *Cldn9*$^{+/+}$ vs. *Cldn9*$^{+/T}$ at 4 months (p=1.1X10^{-6}); *Cldn9*$^{+/+}$ (4 months) vs. *Cldn9*$^{+/T}$ (8 months) (p=2.3X10^{-6}); are significantly different.

Acknowledgements

We thank members of our laboratory for their comments on this manuscript. This work was supported by grants from the National Institutes of Health (DC016099, DC05135, AG051443, DC015252, and AG060504) to E.N.Y.

Additional information

Author Contributions

E.N.Y and BF designed the research, Y.C. M.C.P.F., J.H.L, J.L, S.P, M.K, B.P, J.K, J.C, L.L, MAG, and E.N.Y., analyzed data and wrote the manuscript. All authors read and approved the final manuscript.

Note

This reviewed preprint has been updated to correct the affiliations.

References

Atkinson P.J., Wise A.K., Flynn B.O., Nayagam B.A., Richardson R.T (2014) **Hair cell regeneration after ATOH1 gene therapy in the cochlea of profoundly deaf adult guinea pigs** *PloS one* **9**:e102077 Google Scholar

Bermingham N.A., Hassan B.A., Price S.D., Vollrath M.A., Ben-Arie N., Eatock R.A., Bellen H.J., Lysakowski A., Zoghbi H.Y (1999) **Math1: an essential gene for the generation of inner ear hair cells** *Science* **284**:1837–1841 Google Scholar

Bhat A.A., Syed N., Therachiyil L., Nisar S., Hashem S., Macha M.A., Yadav S.K., Krishnankutty R., Muralitharan S., Al-Naemi H (2020) **Claudin-1, a double-edged sword in cancer** *International journal of molecular sciences* **21**:569 Google Scholar

Brooker R., Hozumi K., Lewis J (2006) **Notch ligands with contrasting functions: Jagged1 and Delta1 in the mouse inner ear** *Development* **133**:1277–1286 Google Scholar

Brown R., Groves A.K (2020) **Hear, Hear for Notch: Control of Cell Fates in the Inner Ear by Notch Signaling** *Biomolecules* **10** Google Scholar

Burns J., Christophel J.J., Collado M.S., Magnus C., Carfrae M., Corwin J.T (2008) **Reinforcement of cell junctions correlates with the absence of hair cell regeneration in mammals and its occurrence in birds** *Journal of Comparative Neurology* **511**:396–414 Google Scholar

Burns J.C., Collado M.S., Oliver E.R., Corwin J.T (2013) **Specializations of intercellular junctions are associated with the presence and absence of hair cell regeneration in ears from six vertebrate classes** *Journal of Comparative Neurology* **521**:1430–1448 Google Scholar

Chen Y., Bielefeld E.C., Mellott J.G., Wang W., Mafi A.M., Yamoah E.N., Bao J (2021) **Early physiological and cellular indicators of cisplatin-induced ototoxicity** *Journal of the Association for Research in Otolaryngology* **22**:107–126 Google Scholar

Chrysostomou E., Gale J.E., Daudet N (2012) **Delta-like 1 and lateral inhibition during hair cell formation in the chicken inner ear: evidence against cis-inhibition** *Development* **139**:3764–3774 Google Scholar

Cohen-Salmon M., Ott T., Michel V., Hardelin J.P., Perfettini I., Eybalin M., Wu T., Marcus D.C., Wangemann P., Willecke K., et al. (2002) **Targeted ablation of connexin26 in the inner ear epithelial gap junction network causes hearing impairment and cell death** *Curr Biol* **12**:1106–1111 Google Scholar

Corwin J.T., Jones J.E., Katayama A., Kelley M.W., Warchol M.E. (2007) **Hair cell regeneration: the identities of progenitor cells, potential triggers and instructive cues** In: *Ciba Foundation Symposium 160-Regeneration of Vertebrate Sensory Receptor Cells: Regeneration of Vertebrate Sensory Receptor Cells: Ciba Foundation Symposium* Wiley Online Library Google Scholar

Daudet N., Lewis J (2005) **Two contrasting roles for Notch activity in chick inner ear development: specification of prosensory patches and lateral inhibition of hair-cell differentiation** *Development* **132**:541–551 Google Scholar

Díaz-Coránguez M., Liu X., Antonetti D.A (2019) **Tight junctions in cell proliferation** *International Journal of Molecular Sciences* **20**:5972 Google Scholar

Dou H., Vazquez A.E., Namkung Y., Chu H., Cardell E.L., Nie L., Parson S., Shin H.S., Yamoah E.N (2004) **Null mutation of alpha1D Ca2+ channel gene results in deafness but no vestibular defect in mice** *J Assoc Res Otolaryngol* **5**:215–226 Google Scholar

Fairchild M.J., Yang L., Goodwin K., Tanentzapf G (2016) **Occluding Junctions Maintain Stem Cell Niche Homeostasis in the Fly Testes** *Curr Biol* **26**:2492–2499 Google Scholar

Gale J.E., Marcotti W., Kennedy H.J., Kros C.J., Richardson G.P (2001) **FM1-43 dye behaves as a permeant blocker of the hair-cell mechanotransducer channel** *J Neurosci* **21**:7013–7025 Google Scholar

Garcia-Anoveros J., Clancy J.C., Foo C.Z., Garcia-Gomez I., Zhou Y., Homma K., Cheatham M.A., Duggan A (2022) **Tbx2 is a master regulator of inner versus outer hair cell differentiation** *Nature* **605**:298–303 Google Scholar

Goodyear R., Richardson G (1997) **Pattern formation in the basilar papilla: evidence for cell rearrangement** *Journal of Neuroscience* **17**:6289–6301 Google Scholar

Gubbels S.P., Woessner D.W., Mitchell J.C., Ricci A.J., Brigande J.V (2008) **Functional auditory hair cells produced in the mammalian cochlea by in utero gene transfer** *Nature* **455**:537–541 Google Scholar

Hinton A.S., Yang-Hood A., Schrader A.D., Loose C., Ohlemiller K.K., McLean W.J (2021) **Approaches to Treat Sensorineural Hearing Loss by Hair-Cell Regeneration: The Current State of Therapeutic Developments and Their Potential Impact on Audiological Clinical Practice** *Journal of the American Academy of Audiology* **32**:661–669 Google Scholar

Hong L., Wu Y., Feng J., Yu S., Li C., Wu Y., Li Z., Cao L., Wang F., Zhang Y (2014) **Overexpression of the cell adhesion molecule claudin-9 is associated with invasion in pituitary oncocytomas** *Human Pathology* **45**:2423–2429 Google Scholar

Hudspeth A.J (2008) **Making an effort to listen: mechanical amplification in the ear** *Neuron* **59**:530–545 Google Scholar

Iyer A.A., Hosamani I., Nguyen J.D., Cai T., Singh S., Beyer L., Zhang H., Jen H.-I., Yousaf R., Birol O (2022a) **Cellular reprogramming with ATOH1, GFI1, and POU4F3 implicate epigenetic changes and cell-cell signaling as obstacles to hair cell regeneration in mature mammals** *bioRxiv* Google Scholar

Iyer A.A., Hosamani I., Nguyen J.D., Cai T., Singh S., McGovern M.M., Beyer L., Zhang H., Jen H.-I., Yousaf R (2022b) **Cellular reprogramming with ATOH1, GFI1, and POU4F3 implicate epigenetic changes and cell-cell signaling as obstacles to hair cell regeneration in mature mammals** *Elife* **11**:e79712 Google Scholar

Izumikawa M., Minoda R., Kawamoto K., Abrashkin K.A., Swiderski D.L., Dolan D.F., Brough D.E., Raphael Y (2005) **Auditory hair cell replacement and hearing improvement by Atoh1 gene therapy in deaf mammals** *Nat Med* **11**:271–276 Google Scholar

Jahan I., Pan N., Kersigo J., Fritzsch B (2015) **Neurog1 can partially substitute for Atoh1 function in hair cell differentiation and maintenance during organ of Corti development** *Development* **142**:2810–2821 Google Scholar

Jeon S.J., Fujioka M., Kim S.C., Edge A.S (2011) **Notch signaling alters sensory or neuronal cell fate specification of inner ear stem cells** *J Neurosci* **31**:8351–8358 Google Scholar

Kaiser M., Ludtke T.H., Deuper L., Rudat C., Christoffels V.M., Kispert A., Trowe M.O (2022) **TBX2 specifies and maintains inner hair and supporting cell fate in the Organ of Corti** *Nat Commun* **13**:7628 Google Scholar

Kimitsuki T., Nishida M., Kawano H., Haruta A., Matsuda K., Komune S (2001) **Membrane current possessing the properties of a mechano-electric transducer current in inner hair cells of guinea-pig cochlea** *Brain Res* **915**:101–103 Google Scholar

Kitajiri S.-i., Furuse M., Morita K., Saishin-Kiuchi Y., Kido H., Ito J., Tsukita S. (2004) **Expression patterns of claudins, tight junction adhesion molecules, in the inner ear** *Hearing research* **187**:25–34 Google Scholar

Kitajiri S., Katsuno T (2016) **Tricellular Tight Junctions in the Inner Ear** *Biomed Res Int* **2016**:6137541 Google Scholar

Kudo T., Wangemann P., Marcus D.C (2018) **Claudin expression during early postnatal development of the murine cochlea** *BMC physiology* **18**:1–8 Google Scholar

Lanford P.J., Lan Y., Jiang R., Lindsell C., Weinmaster G., Gridley T., Kelley M.W (1999) **Notch signalling pathway mediates hair cell development in mammalian cochlea** *Nature genetics* **21**:289–292 Google Scholar

Lewis J (1998) **Notch signalling and the control of cell fate choices in vertebrates** *Semin Cell Dev Biol* **9**:583–589 Google Scholar

Li S., He S., Lu Y., Jia S., Liu Z (2023) **Epistatic genetic interactions between Insm1 and Ikzf2 during cochlear outer hair cell development** *Cell Rep* **42**:112504 Google Scholar

Liu Z., Dearman J.A., Cox B.C., Walters B.J., Zhang L., Ayrault O., Zindy F., Gan L., Roussel M.F., Zuo J (2012) **Age-dependent in vivo conversion of mouse cochlear pillar and Deiters' cells to immature hair cells by Atoh1 ectopic expression** *Journal of Neuroscience* **32**:6600–6610 Google Scholar

Lowenheim H., Furness D.N., Kil J., Zinn C., Gultig K., Fero M.L., Frost D., Gummer A.W., Roberts J.M., Rubel E.W., et al. (1999) **Gene disruption of p27(Kip1) allows cell proliferation in the postnatal and adult organ of corti** *Proc Natl Acad Sci U S A* **96**:4084–4088 Google Scholar

Mathern D.R., Laitman L.E., Hovhannisyan Z., Dunkin D., Farsio S., Malik T.J., Roda G., Chitre A., Iuga A.C., Yeretssian G., et al. (2014) **Mouse and human Notch-1 regulate mucosal immune responses** *Mucosal Immunol* **7**:995–1005 Google Scholar

Mizutari K., Fujioka M., Hosoya M., Bramhall N., Okano H.J., Okano H., Edge A.S (2013) **Notch inhibition induces cochlear hair cell regeneration and recovery of hearing after acoustic trauma** *Neuron* **77**:58–69 Google Scholar

Montalbano G., Olivotto I., Germanà A., Randazzo B (2021) **Evaluation of the hair cell regeneration and claudin b and phoenix gene expression during exposure to low concentrations of cadmium and zinc in early developing zebrafish larvae** *Comparative Biochemistry and Physiology Part C: Toxicology & Pharmacology* **248**:109116 Google Scholar

Montgomery S.C., Cox B.C (2016) **Whole mount dissection and immunofluorescence of the adult mouse cochlea. JoVE (Journal of Visualized Experiments)** *e* **53561** Google Scholar

Muniak M.A., Rivas A., Montey K.L., May B.J., Francis H.W., Ryugo D.K (2013) **3D model of frequency representation in the cochlear nucleus of the CBA/J mouse** *Journal of Comparative Neurology* **521**:1510–1532 Google Scholar

Nakano Y., Kim S.H., Kim H.-M., Sanneman J.D., Zhang Y., Smith R.J., Marcus D.C., Wangemann P., Nessler R.A., Bánfi B (2009) **A claudin-9–based ion permeability barrier is essential for hearing** *PLoS genetics* **5**:e1000610 Google Scholar

Neitzel R.L., Fligor B.J (2019) **Risk of noise-induced hearing loss due to recreational sound: Review and recommendations** *The Journal of the Acoustical Society of America* **146**:3911–3921 Google Scholar

Pangrsic T., Lasarow L., Reuter K., Takago H., Schwander M., Riedel D., Frank T., Tarantino L.M., Bailey J.S., Strenzke N., et al. (2010) **Hearing requires otoferlin-dependent efficient replenishment of synaptic vesicles in hair cells** *Nat Neurosci* **13**:869–876 Google Scholar

Peguero B., Tempel B.L (2015) **A chromosome 17 locus engenders frequency-specific non-progressive hearing loss that contributes to age-related hearing loss in mice** *Journal of the Association for Research in Otolaryngology* **16**:459–471 Google Scholar

Petrovic J., Formosa-Jordan P., Luna-Escalante J.C., Abelló G., Ibañes M., Neves J., Giraldez F (2014) **Ligand-dependent Notch signaling strength orchestrates lateral induction and lateral inhibition in the developing inner ear** *Development* **141**:2313–2324 Google Scholar

Roux I., Safieddine S., Nouvian R., Grati M., Simmler M.C., Bahloul A., Perfettini I., Le Gall M., Rostaing P., Hamard G., et al. (2006) **Otoferlin, defective in a human deafness form, is essential for exocytosis at the auditory ribbon synapse** *Cell* **127**:277–289 Google Scholar

Rybak L., Ramkumar V (2007) **Ototoxicity** *Kidney international* **72**:931–935 Google Scholar

Schwander M., Sczaniecka A., Grillet N., Bailey J.S., Avenarius M., Najmabadi H., Steffy B.M., Federe G.C., Lagler E.A., Banan R (2007) **A forward genetics screen in mice identifies recessive deafness traits and reveals that pejvakin is essential for outer hair cell function** *Journal of Neuroscience* **27**:2163–2175 Google Scholar

Senften M., Schwander M., Kazmierczak P., Lillo C., Shin J.-B., Hasson T., Géléoc G.S., Gillespie P.G., Williams D., Holt J.R (2006) **Physical and functional interaction between protocadherin 15 and myosin VIIa in mechanosensory hair cells** *Journal of Neuroscience* **26**:2060–2071 Google Scholar

Sergeyenko Y., Lall K., Liberman M.C., Kujawa S.G (2013) **Age-related cochlear synaptopathy: an early-onset contributor to auditory functional decline** *J Neurosci* **33**:13686–13694 Google Scholar

Stone J.S., Rubel E.W (1999) **Delta1 expression during avian hair cell regeneration** *Development* **126**:961–973 Google Scholar

Strenzke N., Chakrabarti R., Al-Moyed H., Muller A., Hoch G., Pangrsic T., Yamanbaeva G., Lenz C., Pan K.T., Auge E., et al. (2016) **Hair cell synaptic dysfunction, auditory fatigue and thermal sensitivity in otoferlin Ile515Thr mutants** *EMBO J* **35**:2519–2535 Google Scholar

Sullivan C.B., Al-Qurayshi Z., Zhu V., Liu A., Dunn C., Gantz B.J., Hansen M.R (2020) **Long-term audiologic outcomes after cochlear implantation for single-sided deafness** *Laryngoscope* **130**:1805–1811 Google Scholar

Sun S., Babola T., Pregernig G., So K.S., Nguyen M., Su S.M., Palermo A.T., Bergles D.E., Burns J.C., Muller U (2018) **Hair Cell Mechanotransduction Regulates Spontaneous Activity and Spiral Ganglion Subtype Specification in the Auditory System** *Cell* **174**:1247–1263 Google Scholar

Tang P.C., Chen L., Singh S., Groves A.K., Koehler K.R., Liu X.Z., Nelson R.F (2023) **Early Wnt Signaling Activation Promotes Inner Ear Differentiation via Cell Caudalization in Mouse Stem Cell-Derived Organoids** *Stem Cells* **41**:26–38 Google Scholar

Von Bekesy G. (1952) **Resting potentials inside the cochlear partition of the guinea pig** *Nature* **169**:241–242 Google Scholar

Waqas M., Zhang S., He Z., Tang M., Chai R (2016) **Role of Wnt and Notch signaling in regulating hair cell regeneration in the cochlea** *Frontiers of medicine* **10**:237–249 Google Scholar

White P.M., Doetzlhofer A., Lee Y.S., Groves A.K., Segil N (2006) **Mammalian cochlear supporting cells can divide and trans-differentiate into hair cells** *Nature* **441**:984–987 Google Scholar

Willott J.F., Erway L.C (1998) **Genetics of age-related hearing loss in mice. IV. Cochlear pathology and hearing loss in 25 BXD recombinant inbred mouse strains** *Hear Res* **119**:27–36 Google Scholar

Wilson B.S., Tucci D.L (2021) **Addressing the global burden of hearing loss** *The Lancet* **397**:945–947 Google Scholar

Wu P.-z., O'Malley J.T., de Gruttola V., Liberman M.C. (2020) **Age-related hearing loss is dominated by damage to inner ear sensory cells, not the cellular battery that powers them** *Journal of Neuroscience* **40**:6357–6366 Google Scholar

Yang J., Bouvron S., Lv P., Chi F., Yamoah E.N (2012) **Functional features of trans-differentiated hair cells mediated by Atoh1 reveals a primordial mechanism** *J Neurosci* **32**:3712–3725 Google Scholar

Zavala-Zendejas V.E., Torres-Martinez A.C., Salas-Morales B., Fortoul T.I., Montaño L.F., Rendon-Huerta E.P (2011) **Claudin-6, 7, or 9 overexpression in the human gastric adenocarcinoma cell line AGS increases its invasiveness, migration, and proliferation rate** *Cancer Investigation* **29**:1–11 Google Scholar

Zheng J.L., Gao W.-Q (2000) **Overexpression of Math1 induces robust production of extra hair cells in postnatal rat inner ears** *Nature Neuroscience* **3**:580–586 Google Scholar

Zine A., Messat Y., Fritzsch B (2021) **A human induced pluripotent stem cell-based modular platform to challenge sensorineural hearing loss** *Stem Cells* **39**:697–706 Google Scholar

Zine A., Van De Water T.R., de Ribaupierre F. (2000) **Notch signaling regulates the pattern of auditory hair cell differentiation in mammals** *Development* **127**:3373–3383 Google Scholar

Author information

Yingying Chen*
University of Nevada, Reno, School of Medicine, Department of Physiology and Cell Biology, Reno, United States, Indiana University School of Medicine, Department of Pharmacology and Toxicology, Indianapolis, United States

*Authors contributed equally and are co-first authors.

Jeong Han Lee*
University of Nevada, Reno, School of Medicine, Department of Physiology and Cell Biology, Reno, United States

*Authors contributed equally and are co-first authors.

Jin Li
Department of Otolaryngology, University of Washington, Seattle, United States

Seojin Park
University of Nevada, Reno, School of Medicine, Department of Physiology and Cell Biology, Reno, United States, Prestige Biopharma, Busan, Republic of Korea

Maria C Perez Flores
University of Nevada, Reno, School of Medicine, Department of Physiology and Cell Biology, Reno, United States

Braulio Peguero
Department of Otolaryngology, University of Washington, Seattle, United States

Jennifer Kersigo
University of Iowa, Department of Biology, Iowa City, United States

Mincheol Kang
University of Nevada, Reno, School of Medicine, Department of Physiology and Cell Biology, Reno, United States, Prestige Biopharma, Busan, Republic of Korea

Jinsil Choi
University of Nevada, Reno, School of Medicine, Department of Physiology and Cell Biology, Reno, United States

Lauren Levine
Boys town National Research Hospital, Omaha, United States, Washington University, Program in Audiology and Communication Sciences, Seattle, United States

Michael Anne Gratton
Boys town National Research Hospital, Omaha, United States

Bernd Fritzsch
University of Iowa, Department of Biology, Iowa City, United States

Ebenezer N Yamoah*
University of Nevada, Reno, School of Medicine, Department of Physiology and Cell Biology, Reno, United States
ORCID iD: 0000-0002-9797-085X

For correspondence: enyamoah@gmail.com
*Authors contributed equally and are co-first authors.

Editors

Reviewing Editor
Pascal Martin
Institut Curie, Paris, France

Senior Editor
Barbara Shinn-Cunningham
Carnegie Mellon University, Pittsburgh, United States of America

Reviewer #1 (Public review):

The focus of this manuscript was to investigate the role of Cldn9 in the development of the mammalian cochlea. The main rationale of the study is the fact that cochlear hair cells do not regenerate, so when damaged they are lost forever, causing irreparable hearing loss. The authors have attempted to address this problem by inducing the ectopic production of additional hair cells and test whether they acquire the morphological and functional characteristics of native hair cells. They show that downregulation of Cldn9 using a well-established genetic manipulation of transgenic mice led to the production of extra numerary inner hair cells, which were able to survive for several months. By performing a large battery of experiments, the authors were able to determine that the native and ectopic inner hair cells have comparable morphological and physiological characteristics. There are several conclusions highlighted by the authors in different parts of the manuscript, including the key role of Cldn9 in coordinating embryonic and postnatal development, the differentiation of supporting cells into inner hair cells, and the possible use of Cldn9 to induce inner hair cell differentiation following deafness induced by hair cell loss.

Comments on revised version:

The authors have addressed the following points raised during the first submission: statistical analysis and wave 1 analysis. However, very little was done to address the other key aspects of my report, which are essential for the interpretation of the results. As mentioned in my previous report, some aspects of the work are not justified by the current data and will require either a tone-down of the claims or further experiments.

For example, one puzzling finding that is not addressed in the manuscript is the lack of functional benefit from these additional inner hair cells. In fact, it appears to be detrimental based on the increased ABR thresholds and EP. So, it is not clear to this reviewer the advantage of this approach.

It is not clear what direct evidence there is, apart from some immunostaining, indicating that the ectopic inner hair cells derive from the supporting cells. This part would benefit from a more careful consideration and maybe an attempt at a more direct experimental approach. Alternatively, the text should be modified accordingly.

One point that should be made clear throughout the manuscript is that the ectopic inner hair cells are generated in a cochlea that is undergoing normal maturation. Thus, there is no guarantee that modulating the expression levels of Cldn9 in a deaf mouse lacking hair cells would produce the same result as that shown in this study. This point should be at least discussed.

https://doi.org/10.7554/eLife.92877.2.sa3

Reviewer #3 (Public review):

The study by Chen et al reports an interesting and previously unknown phenomenon of generation of supernumerary inner hair cells (IHCs) in response to downregulation of Cldn9 during embryonic or postnatal development. The authors developed an inducible doxycycline (dox)-tet-OFF-Cldn9 transgenic mice to regulate expression levels of Cldn9 and show that downregulation of Cldn9 resulted in additional, although incomplete row of IHCs immediately adjacent to the original IHC row. These induced extra IHCs had similar well-developed hair bundles, able to mechanotransduce and were innervated by auditory neurons, resembling wild-type IHCs. In addition, the authors knock down Cldn9 postnatally using shRNA injections in P1-7 mice with similar induction of extranumerary IHCs next to the original row of IHCs. The conclusions of this paper are mostly well supported by the data. However, some data analyses are limited, and some important controls are not shown.
The data from this study are important and promising for future gene therapy applications. The generation of extra IHCs postnatally using downregulation of Cldn9 by shRNA could potentially be used as a replacement of IHCs lost after noise-induced trauma, ototoxic agents, or other environmental trauma. However, it is not clear if downregulation of CLDN9 in adult mice would lead to extranumerary IHCs. On the other hand, the replacement of lost inner hair cells due to various genetic mutations by inducing supernumerary mutant IHCs with the same abnormalities would not be reasonable.

The authors show that postnatally generated ectopic IHCs are viable and mechanotransducive, but the hearing function of the mice with ectopic hair cells is not improved. However, the ectopic hair cells seems to be generated from supporting cell trans-differentiation, and the intricate mosaic of the organ of Corti is altered (the extra row of IHCs seems to be positioned immediately adjacent to the original IHC row), which could by itself lead to hearing issues. It is not clear if the newly formed unusual junctions between the ectopic and original IHCs are sufficiently tight to prevent leakage of the endolymph to the basolateral surface of IHCs. Also, it is not clear if the other organ of Corti tight junctions could lose their tightness due to the downregulation of Cldn9, which could over time affect the endocochlear potential and hearing abilities as shown by this study.

Overall, the manuscript could be of interest to scientists working in the inner ear development and regeneration field, and to the hearing researchers in general and perhaps developmental biologists and cell biologists interested in tight junction proteins and their function.

Strength

The methodologies used are solid and convincing. There is a great potential for practical use of these valuable findings and new knowledge on IHC developmental regulation by Cldn9 expression.

Weakness

Some of the data in this study would benefit from showing corresponding negative controls and higher-resolution images of CLDN9 localization, which the authors chose not to show in the revised manuscript. Importantly, CLDN9 immunofluorescence staining data look different from previously published observations and show cytoplasmic staining of supporting cells only and did not show the staining of tight junctions between the OHCs and supporting cells as well as between the IHCs and supporting cells as reported previously (Kitajiri et al., 2004; Nakano et al., 2009, Ramzan et al., 2021). The organ of Corti schematics showing CLDN9 expression reflects the authors' immunostaining data but is unusual considering that CLDN9 localizes to the tight junctions of the reticular lamina as was shown by immuno-EM in this study and described in previous publications (Kitajiri et al., 2004; Nakano et al., 2009, Ramzan et al., 2021). However, the authors did not provide an explanation for these discrepancies in the Discussion of the manuscript.

Also, more detailed investigations would in some instances clarify the data. For example, it is not clear if the downregulation of Cldn9 affects the other genes known to participate in cell fate determination, and why downregulation of Cldn9 expression resulted in production of extranumerary inner hair cells only and not the other cell types, like OHCs, for example.

https://doi.org/10.7554/eLife.92877.2.sa2

Reviewer #4 (Public review):

The work by Yingying Chen, Jeong Han Lee, and co-authors summarizes the morphological and functional outcomes of Cldn9 loss in the inner ear, particularly in the organ of Corti. While the study does not provide mechanistic insights into how the developmental loss of Cldn9 leads to ectopic hair cell formation, the phenomenon itself is curious. The work primarily focuses on a detailed characterization of the ectopic hair cells, which is well done. Despite the lack of mechanistic insights, the study will be of interest to the inner ear field if several major issues with the manuscript are addressed.

(1) The title, "Genetic and pharmacologic alterations of claudin9 levels suffice to induce functional and mature inner hair cells," is misleading. First, both manipulations (knockout and knockdown) are genetic, and no pharmacology is involved. Second, both manipulations are carried out during the embryonic and neonatal periods, and there is no evidence of mature hair cell regeneration in this study. The title should be revised to reflect this. A more accurate title could be: "Developmental loss of Cldn9 results in functional ectopic inner hair cells that persist through adulthood."
(2) Contact-mediated lateral inhibition in hair cell fate determination is one of the most well-studied phenomena in the inner ear field, and numerous groups have shown that it is mediated by Notch signaling. This must be added to the introduction.
(3) A large body of literature has demonstrated that Notch inhibition alone is not sufficient to regenerate hair cells in adult mice. Therefore, if the loss of claudins disrupts Notch signaling-the proposed mechanisms in the discussion - it is unlikely to be a viable therapeutic strategy for hair cell regeneration in the adult ear. Furthermore, no hair cell ablation experiments were conducted to demonstrate what could be considered true regeneration. These speculative statements should be removed or revised accordingly.

(4) Cldn9 is a tight junction protein and should localize to the membrane. Yet, the data presented show what appears to be diffuse cytoplasmic staining, which is concerning.

https://doi.org/10.7554/eLife.92877.2.sa1

Author response:

The following is the authors' response to the original reviews.

> ***Reviewer #1 (Public Review):***
>
> *Summary:*
>
> *The focus of this manuscript was to investigate the role of Cldn9 in the development of the mammalian cochlea. The main rationale of the study is the fact that cochlear hair cells do not regenerate, so when damaged they are lost forever, causing irreparable hearing loss. The authors have attempted to address this problem by inducing the ectopic production of additional hair cells and testing whether they acquire the morphological and functional characteristics of native hair cells. They show that downregulation of Cldn9 using a well-established genetic manipulation of transgenic mice led to the production of extra numerary inner hair cells, which were able to survive for several months. By performing a large battery of experiments, the authors were able to determine that the native and ectopic inner hair cells have comparable morphological and physiological characteristics. There are several conclusions highlighted by the authors in different parts of the manuscript, including the key role of Cldn9 in coordinating embryonic and postnatal development, the differentiation of supporting cells into inner hair cells, and the possible use of Cldn9 to induce inner hair cell differentiation following deafness induced by hair cell loss.*
>
> *Strengths:*
>
> *Several of the conclusions in this study are well supported by the experimental work.*
>
> *Weaknesses:*
>
> *Some aspects of the data and its interpretation needs better explanation and requires further investigation.*
>
> *(1) The Results section is the most difficult part to read and understand. It contains a very limited, and in some places confusing and repetitive, description of the data. Statistical analysis is missing for some of the key data (e.g., ABRs), and in some places the text contradicts the data presented in the figures (e.g., Figure 8). I am sure carefully revising the text would clarify some of these issues.*

We thank the reviewer for the suggestion. We revised parts of the results section and added the statistical analysis to the ABRs and DPOAE (lines 151-159; Page 29, lines 846-880).

> *(2) One puzzling finding that is not addressed in the manuscript is the lack of functional benefit from these additional inner hair cells. In fact, it appears to be detrimental based on the increased ABR thresholds. Maybe it would be useful to analyze the wave 1 characteristics.*

We thank the reviewer for the suggestion. We added the wave 1 characteristics as S8.

> *(3) It is not clear what direct evidence there is, apart from some immunostaining, indicating that the ectopic inner hair cells derive from the supporting cells. This part*

> *would benefit from a more careful consideration and maybe an attempt at a more direct experimental approach.*

We thank the reviewer for the suggestion. We intend to investigate the origin of the ectopic inner hair cells using (for example, a qRT-PCR, sm FISH, etc.) in our future study.

> *(4) One point that should be made clear throughout the manuscript is that the ectopic inner hair cells are generated in a cochlea that is undergoing normal maturation. Thus, there is no guarantee that modulating the expression levels of Cldn9 in a deaf mouse lacking hair cells would produce the same result as that shown in this study. My guess is that it probably won't, but I am sure this could be tested (maybe in the future) using the excellent experimental approach applied in this study.*

That is a great point. We will explore it in our future experiments.

> ***Reviewer #2 (Public Review):***
>
> *Summary:*
>
> *The generation of functional extranumerary inner hair cells (IHCs) in postnatal mice, particularly with virus-mediated knockdown of Cldn9 mRNA expression in the neonatal cochlear duct, is an important observation. It is significant because not many studies exist that report molecular manipulations of the neonatal organ of Corti that result in the generation of new hair cells that remain functional and appear to be intact for an extended time, here more than one year. Overall, this is a carefully conducted study; the observations are clear, and the methods are solid. Two independent methods for reducing the expression of Cldn9 mRNA were used: a conditional transgenic model and AAV-mediated knockdown with shRNA. The lack of a functional explanation of how the reduced expression of Cldn9 specifically leads to the formation of extranumerary IHCs leaves open questions. For example, it is not clear whether there is indeed a fate change happening and whether Cldn9 reduction affects developmental processes. The discussion of how Cldn9 reduction potentially affects Notch signaling, without hard evidence, is handwaving.*
>
> *Strengths:*
>
> *It is a very interesting observation and somewhat unexpected in its specificity for inner hair cells. Using two different approaches to manipulate Cldn9 expression provides a strong experimental foundation. The study is conducted quantitatively and with care.*
>
> *Weaknesses:*
>
> *The lack of mechanistic insight results in an open-ended story where at least the potential interaction of Cldn9 reduction with known and well-characterized signaling pathway components should have been investigated. This missed opportunity limits the scope of the study and should be addressed: How does Cldn9 downregulation affect the expression levels of other known genes linked to hair cell production and cell fate decisions? Quantitative RT-PCR works well for the authors, and comparing the expression of Notch or other known pathway components could provide mechanistic insight.*

We thank the reviewer for the suggestion. We did quantitative RT-PCR to compare the expression of Notch or other known pathway components in our future work. Besides, we used smFISH with ccnd1 probe and cdkn1b probe to detect cyclin D1 and cyclin-dependent kinase inhibitor 1B (p27) separately in the mouse cochlea. GAPDH was selected as a reference gene. The quantification results showed no significant difference between $Cldn9^{+/T}$ mice and $Cldn9^{+/+}$ mice at P2, P7, and P14.

> *It is unclear how P21 inner hair cells were identified for the patch-clamp experiments shown in Fig 4E-H. This is a challenging endeavor without the possibility of using specific markers.*

We did not have a specific marker for IHCs. However, one with experience in hair bundle morphology and knowledge of their location in the epithelia can identify IHCs from the upright microscope.

> *Please also address the numerous minor points outlined below; it will improve the paper's readability.*

Thanks. Please find the point-to-point answers below.

> *Please include page numbers and line numbers in a revised manuscript.*

We include page numbers and line numbers in a revised manuscript.

> ***Reviewer #3 (Public Review):***
>
> *This important study by Chen et al help in advancing our knowledge about the regulation of inner hair cell (IHC) development and revealed the role of Cldn9 in IHC embryonic and postnatal induction by transdifferentiation from the supporting cells. The authors developed an inducible doxycycline (dox)-tet-OFF-Cldn9 transgenic mice to regulate expression levels of Cldn9 and show that downregulation of Cldn9 resulted in additional, although incomplete row of IHCs immediately adjacent to the original IHC row. These induced extra IHCs had similar well developed hair bundles, able to mechanotransduce and were innervated by auditory neurons resembling wild-type IHCs. In addition, the authors knock down Cldn9 postnatally using shRNA injections in P1-7 mice with similar induction of extranumerary IHC next to the original row of IHCs. The conclusions of this paper are mostly well supported by the data, but some data analysis needed to be clarified and some crucial controls should be provided to improve the confidence in the presented results. There is a great potential for practical use of these valuable findings and new knowledge on IHC developmental regulation to design Cldn9 gene therapy in the future.*
>
> *The described by Chen et al mechanisms of extra hair cell generation by suppression of the tight junction protein Cldn9 expression level are very interesting and previously unknown. In particular, the generation of extra IHCs postnatally using downregulation of Cldn9 by shRNA could potentially be very useful as a replacement of HCs lost after noise-induced trauma, ototoxic agents, or other environmental trauma. On the other hand, the replacement of lost hair cells due to various genetic mutations by inducing a supernumerary IHCs with the same abnormalities would not be reasonable.*
>
> *The authors show that postnatally generated ectopic IHCs are viable and mechanotransducive, but it would be nice to show the maturation steps of ectopic IHC during this postnatal period. For example, stereocilia bundles of the ectopic hair cells should mature later than the original IHCs. A few days after viral delivery of shRNA, you should be able to observe immature IHC bundles that unequivocally will define newly generated IHCs. Unfortunately, the authors show only examples of already mature ectopic IHCs at P21 and in 5-6 weeks old mice and at relatively low resolution. Also, during maturation, IHCs usually have transient axo-somatic synapses that are not present in mature IHCs. It would be great to see if, in 5-6 weeks old mouse, the ectopic IHCs still have axo-somatic synapses or not, and if the majority of the ectopic IHCs have*

> *innervation. Some of the data in this study would benefit from showing corresponding controls and some - from higher resolution imaging.*

We appreciate the reviewer's suggestion. The objective of the paper is to report the phenomenon and present the coarse features of the Cldn9-mediated induced ectopic hair cells. The systematic details are for future studies, which are ongoing and out of the current scope.

> *In the mammalian cochlea, each HC is separated from the next by intervening supporting cells, forming an invariant and alternating mosaic along the cochlea's length. Cochlear supporting cells in some conditions can divide and trans-differentiate into HCs, serving as a potential resource for HC differentiation, using transcription and other developmental signaling factors.*
>
> *However, when ectopic hair cells are generated from supporting cell trans-differentiation, the intricate mosaic of the organ of Corti is altered, which could by itself lead to hearing issues. In case of downregulation of Cldn9, the extra row of IHCs seems to be positioned immediately adjacent to the original IHC row. It is not clear if the newly formed unusual junctions between the ectopic and original IHCs are sufficiently tight to prevent leakage of the endolymph to the basolateral surface of IHCs. Also, it is not clear if the other organ of Corti tight junctions could lose their tightness due to the downregulation of Cldn9, which could over time affect the endocochlear potential as shown by this study and hearing abilities.*

There was a slightly increased ABR threshold (5 dB -15 dB) (Fig. 4A) and a decrease in the magnitude of the EP and the rise in the K^+ concentration in the endolymph and perilymph of Cldn9+/T mice compared to from age-matched littermates (S10) indicated there might be a compromised epithelium tight junction. The downregulation of Cldn9 affected the endocochlear potential and hearing abilities ((Fig. 4A, S10) after 2m, suggesting an age-dependent effect. The effective downregulation of Cldn9 would require proper titration of Cldn9 levels to induce extra hair cells with intact epithelial integrity; work may require additional studies.

> *Importantly, CLDN9 immunofluorescence staining data that show cytoplasmic staining of supporting cells should be revisited and the organ of Corti schematics showing CLDN9 expression should be corrected, considering that CLDN9 localizes to the tight junctions of the reticular lamina as was shown by immunoEM in this study and described in previous publications (Kitajiri et al., 2004; Nakano et al., 2009, Ramzan et al., 2021). While the current version of the manuscript will interest scientists working in the inner ear development and regeneration field, it could be more valuable to hearing researchers outside this immediate field and perhaps developmental biologists and cell biologists after proper revision.*

We appreciate the reviewer's comments. We were concerned about the observation, but the results were consistent. Indeed, that was the motivation for performing the immunoEM (S3). A follow-up report may address it further.

> ***Recommendations for the authors:***
>
> ***Reviewer #2 (Recommendations For The Authors):***
>
> *Please address the points I made about the presentation (word choice, inconsistencies in labeling, etc). It ultimately helps a reader to understand and to follow your logic. This is an important observation.*

We corrected the inconsistencies in labeling and addressed the points you suggested.

> *Making the extra effort to investigate a possible interaction between Cldn9 and Notch signaling would substantially increase the significance of the work.*

Thanks for the suggestions. We will explore it in our future work.

> *Minor points:*
>
> *Some sentences would benefit from revision:*
>
> *- The abstract argues that hearing loss is incurable because mammalian hair cells are terminally differentiated (3rd sentence). This is not accurate.*

Mammalian HCs are terminally differentiated by birth, making HC loss challenging to replace.

> *- The second sentence of the second paragraph of the introduction, "Cochlear SCs can divide and trans-differentiate into HCs, serving as a potential resource for HC differentiation, using transcription and developmental signaling factors (White et al., 2006)," should be referenced in the context of the animal's age. This feature of supporting cells is transient and only observed in neonatal mice. The following sentences in the same paragraph would also benefit from being placed into the same context when appropriate.*

We thank the reviewer for the suggestion. These sentences have been corrected.

> *- Introduction: "But functional features of the newly developed HC are circumspect." The authors probably meant "circumspect," but is this the appropriate word? Also, please use the plural of HC = HCs.*

The sentence has been corrected to “but the functional features of the newly developed HCs are circumspect”.

> *- Introduction: Isn't an essential function of tight junctions in the organ of Corti the separation of fluid-filled spaces? Perhaps additional functions of tight junction proteins are unclear, but at least this one function appears clear.*

We thank the reviewer for the suggestion. We added the “additional” before the “function” in this sentence.

> *- Introduction: "using shRNA injection in postnatal (P) days (P1-7) mice." This is a rather vague statement that could be better defined. Perhaps mention that the injections targeted the round window and that an AAV-based method was used. Also, it is not clear from the methods whether the injection needle pierced the round window. Please clarify. Likewise, the methods state that these experiments were conducted in P1-P15 mice, but the main text says P1-P7. Later, in the results section and in the figure legend for Fig 7, the mice are between P1-P7 and P14; the figure itself is labeled with P1 and P14. However, data is presented (Fig 6) for injections at P2, P4, P7, and P14. In the text referring to Fig 6B in the results section, it is stated, "By contrast, the P14-21 inner ear transfected with Cldn9-shRNA produced no detectable increase..." Only data for P2, P4, P7, and P14 injections are presented. These are minor issues, but please check the inconsistencies because they make it difficult to follow.*

We corrected this sentence to “Analogous additional putative IHCs differentiation was observed when Cldn9-shRNA was injected through the round window to postnatal (P) days (P2-7, and P14) mice…”. The label in Fig 7A has been changed to P2-7, and the text referring to Fig 6B in the result section has been changed to “the P14 inner ear transfected with Cldn9-shRNA produced no detectable increase...".

> *- Last statement of the Introduction: "making Cldn9 a viable target for generating transformed IHCs." It is not clear what transformed IHCs are.*

We replaced the transformed with supernumerary.

> *- To understand the Southern Blot analysis in Fig 1E, the location of BstAPI and BamHI restriction sites and the probe need to be illustrated in Fig 1D.*

The restriction sites BstAPI, (Bst), and BamHI (Bam) are indicated (Fig. 1D).

> *- Please define the purple arrows and arrowheads in Fig 1D. What do the different colors for the backbone mean? I see red and green, but also orange and yellow in the floxed allele. In Fig 1F, is "Knock-in" synonymous with homozygote? Would it be clearer to use the nomenclature Cldn9(T/T), Cldn9(T/+), and Cldn9(+/+), which is used later in the text?*

We have made the changes as requested.

> *- Results, first paragraph: "Results of RT-PCR…" This refers to quantitative RT-PCR; please add the word "quantitative."*

Thanks. We added “quantitative” to the sentence.

> *- Results and Fig S1. Is the strong upregulation of Cldn9 mRNA (S1A) also reflected in stronger Cldn9 immunoreactivity?*

Yes, the strong upregulation of Cldn9 mRNA showed higher cldn9 immunoreactivity.

> *- Results, Fig 1. Please add a schematic drawing showing all elements of the inducible gene expression cassette in the final transgenic allele, and please illustrate how the system works. This helps the reader to understand the strong Cldn9 mRNA upregulation in Cldn9(T/T) mice, where expression is likely driven by the CMV promoter and reciprocally, in the presence of doxycycline, the suppression of transcription by binding of the tTA-dox protein to the TRE elements of the modified CMV promoter. Is this a correct assumption?*

Yes, this is a correct assumption

> *- Results, about Fig S3. Why is it important to investigate Cldn6 and ILDR1 levels in the context of Cldn9 downregulation? Also, that is meant with "no comparative differences in others?". If a potential compensatory effect is suspected, why are the authors not systematically characterizing the expression of other tight junction proteins with quantitative RT-PCR? The results shown in S3 are anecdotal, without proper quantification, and lack context.*

The goal is to examine the potential compensatory changes in other TJ proteins. It was not to examine all possible TJ proteins localized in the inner ear.

> *Results, section headed with "Downregulation of..." First sentence. Fig. 2A-C à Fig. 2A-E.*

Thanks. We corrected the sentence “5-week-old mice *Cldn9*$^{+/T}$ cochleae displayed a notable row of ectopic HCs (Fig. 2A-C).” to “5-week-old mice *Cldn9*$^{+/T}$ cochleae displayed a notable row of ectopic HCs (Fig. 2A-E).”

> *The same section: "were negatively labeled with anti-prestin antibody." Consider "were not labeled with antibody to prestin." Likewise, a few sentences below, please consider rephrasing "the ectopic HCs ... reacted positively to otoferlin antibodies". Also, "...expressed multiple CtBP2 labeling..." - this reads like an incomplete sentence.*

Thanks for the suggestions. We have corrected the three sentences mentioned.

> *The phrase "putative ectopic" lacks clarity because "putative" could refer to "ectopic" (like an adverb). Consider swapping the two words and writing "ectopic putative IHCs" or simply "ectopic IHCs."*

Thanks for the suggestions. We replaced the “putative ectopic IHCs” with “ectopic IHCs” in all contexts.

> *Please use more precise figure labels when referring to a specific figure panel. For example, "Additionally, the ectopic HCs show IHC bundle features (Fig. 2)," - Bundles are shown in Fig 2D and Fig 2E. Please check all instances where a full figure is mentioned, but the specific reference is to a panel of the figure. Another example, "... using quantitative RT-PCR (S7)..." would be more specific if Fig S7A is referred to.*

Thanks for the suggestions. We checked all instances and corrected the labels. Thanks!

> *"IHC counts at different ages (P2-P21) and the cochlear frequency segments (4-32 kHz) demonstrate..."- the figure shows data for 8 kHz and 32 kHz; please revise: "segments (8 kHz and 32 kHz) demonstrate."*

This sentence has been revised based on your suggestion. Thanks!

> *Please add a legend to Fig. 3C (like the one shown in Fig. 2F).*

Thanks for the reminder. The legend for Fig. 3C was modified.

> *Fig 4A and Fig 4B. It is impossible to distinguish the open/closed circles and the many lines. Please consider a different format or an extended supplemental figure. Also, drawing a line connection between the 32 kHz and click data points in 4A is inappropriate.*

Instead of the open/closed circles, the dashed line means *Cldn9*$^{+/+}$ mice, and solid lines represent *Cldn9*$^{+/T}$ mice. We added the line labels. The line connecting between 32 kHz and click data points was removed.

> *Fig 4, legend. Please define BHB and BHC levels.*

BHB and BHC are defined.

> *The paragraph "Synaptic features of PE IHCs match original IHCs" is confusing because it states the following: "The synapses between the IHCs and auditory neurons at the apical,*

> *middle, and basal cochlear locations from 5-week-old Cldn9+/+ and Cldn9+/T mice show substantial differences." The meaning of the heading, therefore, does not match what is ultimately shown and discussed.*

We have changed the title to “Synaptic features of ectopic IHCs and original IHCs”.

> *Moreover, no actual features of synapses are investigated; CtBP2/Homer pairs were used to identify afferent synapses, which this reviewer would argue provides a reasonable estimate of the number of synapses where pre- and post-synaptic markers are detected in close vicinity. It would be helpful to describe the method for counting juxtaposed CtBP2 and Homer-labeled puncta with more detail.*

The method section now includes more information about the synapse count, which this reviewer would argue provides a reasonable estimate of the number of synapses where pre- and post-synaptic markers are detected in close proximity.

> *The final concluding sentence of the section also suggests that synaptic transmission from PE IHCs might be compromised because significant differences in synapse numbers were identified. It would be important to mention this.*

Thanks for the reminder. We added this information to the final concluding sentence.

> *Fig. 5C, 5D; legend. Is "co-expressed" the right word choice? Consider "colocalized" or "juxtaposed".*

The "co-expressed" has been replaced with "colocalized".

> *Voltage-clamp recordings of P21 inner hair cell mechanoelectrical transduction currents. This reviewer cannot identify a previous publication describing the details of this method on P21 cochlear inner hair cells; this seems like an excellent methodological advance.*

Yes, we can record data from older mice. Thanks for pointing it out.

> *"Transfection in vivo of Cldn9 shRNA," the P14-21 inner ear transfected with Cldn9-shRNA." Plus, additional use of the word "transfection." Transfection generally means the introduction of plain nucleic acid into cells. The word refers to methods that do not use viruses. In contrast, "transduction" is the term used for virus-mediated gene transfer. The authors used AAVs. Please correct for appropriate scientific terminology.*

Thanks for the clarification. This information has been corrected accordingly.

> *"A slight decline in the amplitude of the EP and a substantial rise in perilymph K+ was detected in 8-month-old Cldn9+/T (S7)." Probably Fig. S8A,B is meant.*

Yes, it referred to Fig. S8 A, B. We corrected it in the result section. Thanks!

> *Heading "Discussions" -> "Discussion"*
>
> *The focus of the second part of the discussion on potential interactions between Cldn9 suppression and known signaling pathways is essential. The logic that is presented with respect to Notch signaling, however, is not clear and misleading. For example, it is not obvious what is meant by "Cldn9 subserves the signaling catalyst to activate NICD cascades" and whether this statement is supported by any published data.*

The statement was a suggestion and has been qualified with a “may” clause (line 299).

> *The authors might consider discussing whether the observed effect caused by Cldn9 elimination is a specific role of the Cldn9 protein itself or is an epiphenomenon resulting from cytomechanical changes in the developing and maturing organ of Corti. This would add a potential Notch-independent component for a possible interpretation of the observations.*

We state lines 302-304 “Alternatively, *Cldn9* levels disruption may alter the mechanical properties of the developing and maturing organ of Corti that may trigger ectopic IHC differentiation, an epiphenomenon independent of the Notch signaling“.

> *Methods:*
>
> *"Deletion of the selection marker in the tTA cassette by crossing the F1 mouse with the embryonic Cre line (B6.129S4-Meox2tm1(cre)Sor/J)." This sentence seems to be incomplete.*

Thanks for pointing it out. This sentence has been rewritten.

> *"Images were captured under a confocal microscope." Consider writing "with a confocal microscope".*

This sentence has been corrected. Thanks!

> *RNA extraction and... How many mice were used per experiment? 10-15 or just 10?*

The mice number for the RNA extraction is between 10 and 15. Thanks

> ***Reviewer #3 (Recommendations For The Authors):***
>
> *Below are my suggestions, questions, and criticisms.*
>
> *(1) The red outline on Fig1A schematic does not correspond to the previously published expression pattern of CLDN9 in the organ of Corti reticular lamina tight junctions (Kitajiri et al, 2004, Nakano et al., 2009, Ramzan et al., 2021). Also, there are no tight junctions all around the pillar cells. The tight junctions are restricted to the sites of tight attachments between two cells. The immunofluorescence staining using CLDN9 antibody looks rather cytoplasmic (Fig 1 and Fig S1) than associated with the tight junctions as it was shown by immunoEM data here and reported previously (Kitajiri et al, 2004; Nakano et al, 2009; Ramzan et al, 2021). Please correct the schematic and explain your data.*

We have redrawn the diagram (Fig. 7).

> *(2) The CLDN9 staining in Figure 1, B and C, highlights the cytoplasm of the supporting cells, and hair cells devoid of the staining. From the images in Fig. S1C, it also looks like CLDN9 is present only in supporting cells and not in hair cells? How would the authors reconcile their data with Cldn9 expression data from the gEAR database and Ramzan et al.'s 2021 RNAscope data? Please provide the validation of the antibody used in this study.*

We recognize the reviewer’s concern but RNA and protein levels are not always in parallel.

> *(3) Figure 1D. The dash lines from the targeting vector to the wt allele seem to indicate a recombination event. Please do not show the recombination event, instead just show what part of the targeting vector was incorporated to replace wt Cldn9. There is no description in the figure 1 legend what purple arrows and arrowheads mean and what yellow and orange line segments in the floxed allele schematic indicate. Please also show where the BstAPI and BamHI restriction enzyme sites are.*

We have provided supplement Fig 1., and have noted the BstAPI and BamHI restriction enzyme sites in Fig. 1D.

> *(4) What does the organ of Corti that has 40-to-55-fold increase in Cldn9 mRNA expression looks like before dox treatment? Any abnormalities at all? How is CLDN9 protein localization looks in the Cldn9+/T untreated mice? Do they have normal number of IHCs? Cldn9+/T untreated mice should be used as another control at least in Figure S1. What does the organ of Corti that has a 40-to-55-fold increase in Cldn9 mRNA expression look like before dox treatment? Are there any abnormalities at all?*

The untreated *Cldn9*$^{+/T}$ mice can grow normally but are not fertile. So, we used a very low concentration of dox water (0.1 mg/ml) instead of normal water to keep the breeding pairs. The protein level increased in the *Cldn9*$^{+/T}$ mice compared with *Cldn9*$^{+/+}$mice. With 0.1 mg/ml dox water, they also showed ectopic IHCs.

> *(5) It is interesting that decline of 0.4-0.6-fold in mRNA level leads to about 8-fold decrease in protein level based on your immunoEM data on tight junctions of IHC with supporting cells. Do you observe the same effect in OHC-SC tight junctions, or the decrease was observed selectively around IHCs?*

The reviewer is alluding to matching RNA and protein levels. It appears that for Clnd9 one cannot expect a closely matched relationship.

> *(6) The quality of the immunoEM data is great, but a control of secondary antibody alone staining in wt and Cldn9+/T dox treated should be shown and compared to the Cldn9+/T treated sample.*

We thank the reviewer for raising the issue. Secondary antibodies are used as a control in all immunoEMs in the laboratory. We opted not to show negative results.

> *(7) The authors observed a decrease in Cldn6 expression albeit not quantitative in response to Cldn9 downregulation. How were the immunofluorescence signals compared and evaluated? Please provide a detailed description of the method used. Did the authors used the same image acquisition parameters? Was the Cldn9 and Cldn6 immunostaining done using same protocol with the same aliquot and dilution of the secondary antibodies, etc.? The staining for CLDN6 seems to be concentrated in the cytoplasm of supporting cells, and not in the tight junctions, similar to CLDN9 immunoreactivity shown in Fig. S1C and to the ILDR1 pattern of staining in Fig. S3. How can the authors explain this? How were the antibodies validated?*

The Cldn9 and Cldn6 immunostaining were done using the same protocol with the same aliquot and dilution of the secondary antibodies.

> *(8) CLDN14 is also expressed in the organ of Corti tight junctions. What happened to this TJ protein during CLDN9 downregulation?*

We detected Cldn14 with immunostaining in the *Cldn9+/T* mice and *Cldn9+/+* mice fed with 0.25 mg/ml dox water, and the results showed increased expression of Cldn14 in *Cldn9+/T* mice. Detail alterations of other TJ proteins have been reserved for future studies.

> *(9) When supernumerary IHCs were observed in Cldn9+/T mice, have the authors noticed a corresponding decrease in supporting cells surrounding IHCs? Quantification of the IHCs supporting cells would be useful. Do the ectopic IHCs have apical tight junctions with original IHCs or they are surrounded by supporting cells?*

We quantified the SCs around the IHCs but did not detect significant differences among the groups.

> *(10) The authors indicated that viable PE IHCs were observed in 15 months old Cldn9+/T dox treated mice. How stereocilia bundles look in these ectopic hair cells? Are they preserved similar to the original IHCs or degenerated? It is hard to see this in Fig 3, phalloidin panel. High-resolution SEM would show this better.*

For the remaining ectopic IHCs in 15 months, we did not detect apparent differences in hair bundles compared with the original IHCs.

> *(11) Interestingly, the authors indicate that the highest number of the ectopic IHCs were developed in the apical turn and the higher elevation of ABR threshold was also observed at low frequencies end. This may indicate that extra IHCs do not help hearing function.*

The extra IHCs showed along the whole cochlea, even though it is more obvious in the apical turn. The declined hearing may have resulted from the leakage of the endolymph K+ to the perilymph and EP decline.

> *(12) No age-matched wt control is shown for decreased expression of Cldn9 after shRNA injection at P2 (Fig. 6A).*

As indicated earlier, we opted to state but did not show negative results.

> *(13) Figure 6C. The better- quality SEM images showing a longer stretch of IHCs are needed to convince readers that there are ectopic IHCs that are well preserved in 5-6 weeks old mice in all cochlear turns after GFP-Cldn9 shRNA treatment at P2-P7.*

In S4, we showed that there are ectopic IHCs along the cochlear axis.

> *(14) Do scrambled shRNA control samples had some ectopic IHCs? This control is missing in Fig.6D.*

No scrambled shRNA controls did not show ectopic IHCs. We have stated it.

> *(15) Figure 7B, lower schematic. There are no known continuous tight junctions and CLDN9 expression around the OHCs and IHCs. CLDN9 is known to be concentrated at the reticular lamina tight junctions which separate the endolymph from perilymph. Please, correct all schematics accordingly.*

We have made the changes as requested.

> *Minor comments:*

> *(1) Page 1, Abstract. I would not say "making HC loss incurable" since recent gene therapy results show some advances in this direction. Please rephrase more accurately.*

We have made the changes as requested.

> *(2) Page 4, Results, line 5; please rephrase "PCR of tail tissue samples performed genotyping."*

It has been corrected to “The genotyping was performed by the PCR with the tail tissue.”

> *(3) Fig. 1 legend, panel B, replace "showing IHC stained myosin7a" with "showing IHC stained by myosin7a". Also, in the same sentence, "phalloidin, actin (green) antibodies," Phalloidin is not an antibody; please change this.*

Thanks. We have corrected this information.

> *(4) Fig 2C, IHC label obscures the view of IHCs, please move this label out and use an arrow to point to IHCs.*

We have made the changes as requested.

> *(5) Figure 4, title. Replace "currents elicited original" with "current elicited from original".*

This sentence has been corrected. Thanks.

> *(6) Figure 4, panel A. It is hard to see the open symbols on the graph. Are they associated with the dash lines? Please make them more visible or indicate what dash lines are. "ABR threshold for (n=12)" should be "ABR threshold for Cldn9+/+(n=12)"?*

Yes, they are associated with the dash lines. We added the labels for the solid lines and dash lines. "ABR threshold for (n=12)" was corrected to "ABR threshold for Cldn9+/+(n=12)."

> *(7) Figure 4, legend. "Within each wt and heterozygote mice, there was no significant shift...". Do you mean within each group of mice? Also "Mean DPOAE threshold for 2-8 mos (n=9) was tested,..." Do you mean (n=9) for each group or what group?*

Yes, "Within each wt and heterozygote mice, there was no significant shift..." has been revised. The number of mice in each group for the DPOAE test was clarified in the Fig. 4B legend. Thanks.

> *(8) Please label the X axis in Figure 4D.*

The X-axis has been labeled (Time (s))

> *(9) Figure 4 B, do the colors of the lines indicate the same age groups as in Fig 4A? Do the dash lines associate with open symbols? Please state this clearly in the figure's legend.*

Yes. We added this information in Fig. 4B legend.

> *(10) Figure 4D. Please label the X axis of the fluorescence intensity graph.*

The X-axis has been labeled (Time (s))

> *(11) Figure 4G, legend. Replace "(mean +std)" with "(mean +SD)" for consistency here and in Figure 5 legend.*

Thanks. We replaced "(mean +std)" with "(mean +SD) in the legend of Fig. 4G and Fig.5 and Fig.6.

> *(12) Figure 5B, legend. Replace "makers" with "markers".*

Thanks. This information was corrected.

> *(13) Figure 6A, legend. There is no downregulation of Cldn9 by shRNA shown in "S5". Do the authors mean Figure S7? Please, correct "S5" to "Fig. S7".*

This information was corrected. Thanks.

> *(14) Figure 6A, legend. There is no reduced CLDN9 protein expression shown in Fig. 1C. Do the authors mean Fig. 6A, third panel? Please correct the phrase "reduced protein expression (Fig. 1C) is shown in the 3rd Panel (Cldn9, red)" accordingly, and do not capitalize "p" in the "3rd Panel".*

This information was corrected. Thanks (line 917-918).

> *(15) Also there, replace "The right Panel shows two rows of IHCs (marked HC marker, Myo7a (cyan), and the merged photomicrograph" with "The right panel shows the merged image with two rows of IHCs stained with HC marker Myo7a (cyan) and the expression of Ad-GFP-mCldn9 shRNA (green) in the adjacent row of supporting cells". Please indicate in what cells Ad-GFP-mCldn9 shRNA (green) is expressed. It looks like only one row of supporting cells has this green signal.*

This information was corrected.

> *(16) Figure 6B, legend. Replace "Examples of photomicrographs of sections of the whole-mount cochlea of P2, P4, P7, and P14 Cldn9 shRNA injected mice" with "Examples of phalloidin stained whole-mount organ of Corti samples from cochleae of the wild-type mice injected at P2, P4, P7 and P14 with Cldn9 shRNA"*

This sentence has been modified based on your suggestions. Thanks!

> *(17) Replace "action labeling" with "actin labeled."*

Thanks! The "action labeling" has been replaced with "actin labeled." Line 924

> *(18) Figure 6C. Insert "C" before SEM images description in the legend. The authors stated that SEM images of "5-6-wks-old mice" are shown. Please indicate the exact age of mice shown on each image and at what age these mice received the virus injection.*

Thanks! The “C” has been added. We have noted that the SEM images are from 5-week-old mice" in the legend, and the virus was injected at P2.

> *(19) Figure 6D, legend. Last sentence: move "are significantly different" and insert this between "IHCs" and "at P2 apex".*

This information was corrected.

> *(20) Figure S7, legend. Replace "(sram)" with "(scram)" as in the figure itself. Also, Indicate the age of samples at the harvesting time for imaging and the age at injection of Cldn9 shRNA.*

"(sram)" has been replaced with "(scram)". The age of samples at the harvesting time for imaging and the age at injection of Cldn9 shRNA are indicated.

> *(21) Figure S8. Replace "4 mos-old" and "8 mos-old" with "4 months-old" and "8 months-old" everywhere in the legend and in the figure labels.*

We have made the changes as suggested.

> *(22) Page 8, 5th lane from the bottom. Change "EP and K+ concentration endolymph" to "EP and K+ concentration of the endolymph".*

It has been corrected. Thanks.

> *(23) Page 8, next to the last sentence before the Discussion. Wrong figure number, please replace "(S7)" with "Fig. S8".*

It has been corrected. Thanks.

https://doi.org/10.7554/eLife.92877.2.sa0